МИНИСТЕРСТВО НАУКИ И ВЫСШЕГО ОБРАЗОВАНИЯ
РОССИЙСКОЙ ФЕДЕРАЦИИ

Федеральное государственное автономное
образовательное учреждение высшего образования
«Самарский национальный исследовательский университет
имени академика С.П.Королёва»
(Самарский университет)

Институт ракетно – космической техники

Кафедра технологии металлов и авиационного материаловедения

ВЫПУСКНАЯ КВАЛИФИКАЦИОННАЯ РАБОТА

«СТРУКТУРА И СВОЙСТВА ТЕРМОБАРЬЕРНЫХ ПОКРЫТИЙ, ПОЛУЧЕННЫХ РАЗЛИЧНЫМИ СПОСОБАМИ»

по направлению подготовки 22.04.02 «Металлургия»

(уровень магистратуры)

направленность (профиль) «Инновационные технологии получения и обработки материалов с заданными свойствами»

Студент _____ Х.О. Савалета Т.

Руководитель ВКР,

доцент кафедры ТМиАМ, к.т.н. _____О.С. Бондарева

Самара 2019

МИНИСТЕРСТВО НАУКИ И ВЫСШЕГО ОБРАЗОВАНИЯ
РОССИЙСКОЙ ФЕДЕРАЦИИ

Федеральное государственное автономное
образовательное учреждение высшего образования
«Самарский национальный исследовательский университет
имени академика С.П.Королёва»
(Самарский университет)

Институт ракетно – космической техники
Кафедра технологии металлов и авиационного материаловедения

УТВЕРЖДАЮ

Заведующий кафедрой

_____ С.В. Коновалов

«____» _____ 2019 г.

ЗАДАНИЕ НА ВЫПУСКНУЮ КВАЛИФИКАЦИОННУЮ РАБОТУ МАГИСТРА

студенту _____Савалета Тиснадо, Хонаттан, Омар
группы № _____1239-220402D _____

Тема работы «СТРУКТУРА И СВОЙСТВА ТЕРМОБАРЬЕРНЫХ ПОКРЫТИЙ, ПОЛУЧЕННЫХ РАЗЛИЧНЫМИ СПОСОБАМИ»

Цель работы: исследование микроструктуры и некоторых свойств покрытий, полученных газотермическим плазменным напылением и электро-дуговым пароосаждением в исходном состоянии и после длительной эксплуатации.

Структурные части работы (перечень вопросов, подлежащих разработке): проанализировать условия работы, выбор материала основы и покрытия лопатки турбины; исследовать исходные порошки, используемые для формирования ТЗП, влияние их фракционного состава на структуру покрытия; проанализировать структуру и свойства исходных ТЗП, полученных различными методами осаждения; исследовать и описать структурные изменения в покрытиях, полученных различными методами осаждения, происходящие после длительной эксплуатации лопатки.

Научный руководитель доцент,
кафедра ТМ и АМ
_____ (О.С. Бондарева)
«____» _____ 2019 г.

Задание принял к исполнению

_____ (Х.О. Савалета Т.)
«____»_____ 2019 г.

ABSTRACT

Explanatory note: 78 pages, 48 figures, 15 tables and 68 sources.

THERMAL BARRIER COATING, OVERLAY COATING, DIFFUSION COATING, AIR PLASMA SPRAYING, ELECTRIC ARC PHYSICAL VAPOR DEPOSITION, GAS TURBINE BLADE AND NICKEL SUPERALLOY.

The objective research is evaluated the protective effect of thermal barriers at high temperatures over Nickel superalloy of ZhS6F.

The work purpose - To study the changes in the microstructure of the plasma thermal spray barrier coating and electric arc physical vapor deposition barrier coating, for which the initial state and after the long-term operation were evaluated.

In the work process, the theory of the coatings at high temperatures, the base material of Nickel superalloy, the deposition methods and the analysis methods for the evaluation of the coating are used.

In the work result, the evaluation of each type of coatings system in its initial and final state is presented after being subjected to the operation.

The work effectiveness concludes that the thermal barrier coating system generated by the electric arc physical vapor deposition method, is more effective in protecting the superalloy of ZhS6F at high temperature conditions.

CONTENT

INTRODUCTION

The problem urgency.

The industrial processes that involve operations at high temperatures, where these reach ranges above 1000 °C, as is the case of the gas turbines operation , where your pieces need to be made of materials resistant to this environment. In this materials group stand Nickel's superalloys, which with the help of their components are able to resist these operations, but at frequently operating temperature cycles, these cause wear and degradation of their properties. One way to mitigate these damages is by using barriers, that covering different applications and uses from the study of their properties, how to reinforce them by adding elements in their structure or modifying nanostructurally to improve them , and within them we find the thermal barrier coatings. There are different deposition forms of this coatings type, some of these methods are the air plasma spray and electric arc physical vapor deposition coating, with which two protective layers are formed on the substrate, which fulfill different functions. As a top layer, a ceramic is used, which is composed of yttrium oxide stabilized tetragonal zirconia polycrystals perceives the thermal and erosive effects of the gas flow and reduces the temperature of the blade. Under the ceramic layer is overlay coating such as NiCoCrAlY and/or diffusion coating, which protects the base metal from oxidation and contributes to the adhesion strength of the ceramic layer to the substrate.

When these coatings and the substrate are subjected to destructive effects of the high temperature current, it leads to structural changes in both the layer of the coatings, with the loss of barrier properties; and the formation of the second reaction zone, due to the elements diffusion of the substrate with the bond coat, where harmful closed topologically packed phases (TCP) abound that destroy the mechanical properties of the superalloy.

In the case of the republic of Peru, the industry that involves turbines operating at high temperatures is military and commercial aviation and thermal gas plants. In these industries, the effects of heat on parts of the turbine blades can be harmful, so

the coatings study at high temperatures will be a great help to improve their performance. In the specific case of the thermal power plant sector in 2015 in Peru, a total of 87% of the electricity suppliers were covered; According to data from the Energy Economics Institute, Foundation Bariloche, this led to the increased use and construction of thermal power plants with turbines. In the military aviation case, most of the aircraft are of Russian origin, and maintenance is always carried out by the Peruvian air force, with training or support from various national and foreign agencies. With the study carried out, it will serve to establish the bases for the implementation of this technology in the energy and aviation sector of Peru.

The purpose and research task. To study these effects in the microstructure of the plasma thermal spray barrier coating and arc-electric physical vapor deposition barrier coating, for which the initial state and after the long-term operation were evaluated.

In order to achieve the goal, it is necessary to solve the following tasks:

- Describe the structure and composition of the turbine blade.
- Analyze the initial shape of the coatings, necessary to form the Thermal barrier coating systems.
- Analyze the structure type formed and its properties when generating thermal barrier coating systems, using the aforementioned deposition methods, since each one grants a common characteristic.
- Describe the diffusion of Aluminum by forming the bond coat, which contains overlay coating and diffusion coating and it is the product by electric arc physical vapor deposition method.
- Investigate the formation of the topologically closed packed phases in the turbine blade substrate.
- Investigate the structure of the thermal barrier coating systems after the operation to which they are subjected.
- Investigate the diffusion mechanisms that arise the thermal barrier coating system and the substrate.

Scientific novelty.

- The use of scanning electron microscope TESCAN Vega SB, which allowed to analyze the structures of the coatings and the substrate in their initial stages and subsequent operation. In addition to the composition of the existing elements in the coatings and in the substrate, detecting changes in the composition of some elements, for which it was concluded there is a diffusion of these.

- The use of hardness test, to determine the coatings' hardness according to their structural qualities obtained by the various deposition methods used.

- The section of a thermal barrier coating system obtained by the air plasma spraying method, starting from the alteration of the diameter of the initial coating powders of ZrO_2 + 8% Y_2O_3 used in the top coat while the bond coat is an overlay of NiCoCrAlY coating, with subsequent structural analysis and the hardness of the ceramic coating in the initial conditions.

- The use of MAP-1 equipment, to generate a Thermal Barrier coating system, using the electric arc physical vapor deposition method. For which an overlay coating system (SDP-4) and a diffusion coating (VSDP-16) were used in the bond coat, which contains aluminum in greater proportion, which after being deposited and reheated generates a diffusion of the aluminum, appearing in the bond coat two well-defined zones β-NiAl and the interdiffusion zone. While the top coat was used a ceramic coating of ZrO_2 + 8% Y_2O_3.

1. Alloys and protective coatings for gas turbine engine parts

There are certain materials capable of maintaining their properties at high temperatures, as is the case of heat-resistant materials, the uses of which cover several varieties, among them we find turbines, rockets and heat exchangers.

These materials have three essential characteristics, such as the ability to withstand closed temperature operating loads close to their melting point, for this reason the operating temperature must be taken into account, which must be lower than the melting temperature. The next feature is a substance resistant to mechanical degradation over extended time values for applications of high temperatures, inelasticity and unrecoverable deformation, this is known as "screep", and there being a dependence with thermal activity in high temperature processes. A last characteristic is the tolerance to severe operating environments, this is due to the gases generated are highly corrosive due to the high levels of sulfur in the load [1].

To have arrived at the selection of these materials, technologically the superalloys were developed which are currently linked to the gas turbine engines an example of these engines [2] is the turbojet that corresponds to Figure 1.1. Which is divided into compressor, combustion chamber, turbine and shaft. Each part fulfills a specific function, fundamentally to generate mechanical energy from the fuel (gas) combustion, supporting work at high temperatures.

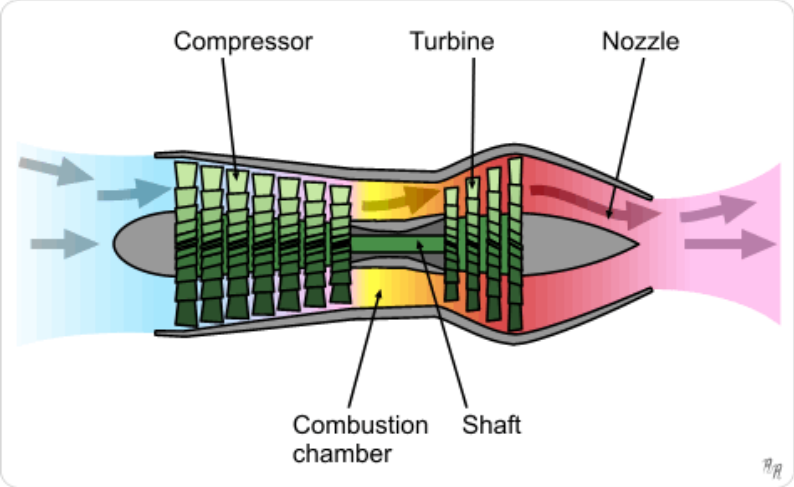

Figure 1.1- Describes the turbojet engine parts and the incoming air temperature change of inside it when it is working [3]

These temperature changes that involve the parts of the turbine, led to the creation of work blades and refrigerated nozzles. Which must counter these effects, also known as the turbine is inlet temperature, since this value is essential for the design of a gas turbine engine. To do this, to design various cooling media, which cover different types: film cooling, convection cooling, steam cooling, full coverage film cooling, impingement cooling, transpiration cooling and multiple small holes cooling design.

The latter is the most effective and used in the blades; since, primary cooling is achieved by film cooling, with the cooling air injected through small holes over the airfoil surface, leading to temperature distribution over the entire surface, this correspond Figure 1.2. The temperature distribution as seen in the figure shows the uncooled values and the cooled values in brackets over the surface of the blades [4].

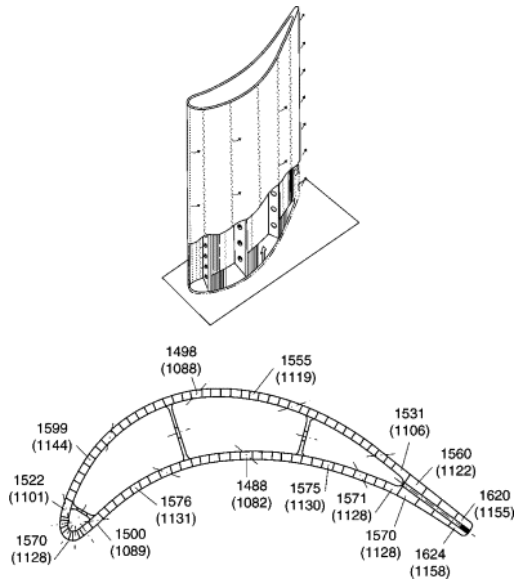

Figure 1.2- Multiples small holes cooling design [4]

Also in the correspond to Figure 1.3, the maximum temperature gradients occur at the transition points of the blade surface at the leading and trailing edge; reducing in the pressure side and suction side [5].

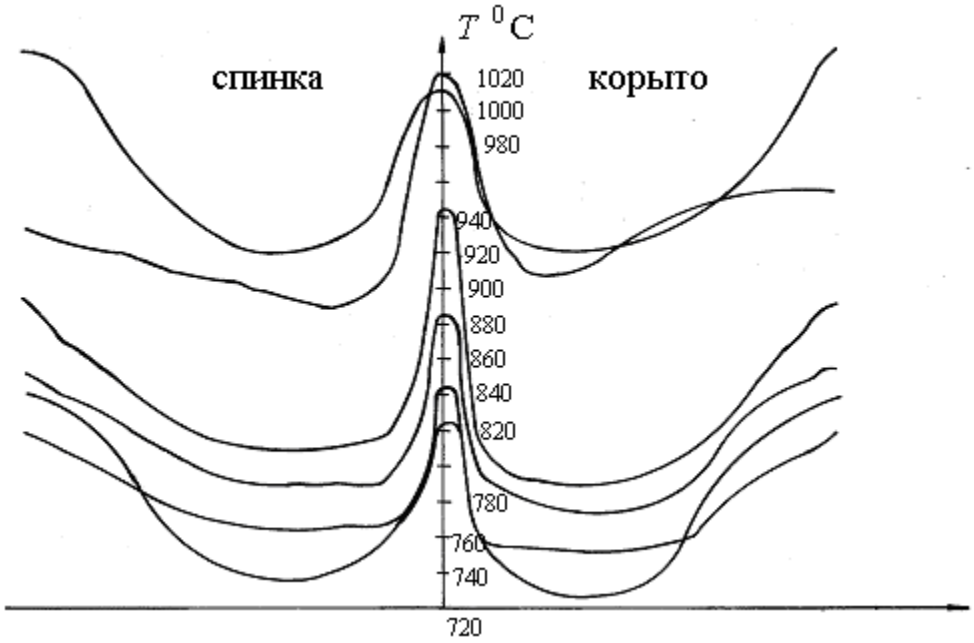

Figure 1.3 - The temperature distribution over surface of a gas turbine blade [5]

In the 20th century, it was a period concentrated in superalloys [6], developing processes for their performance. Because appearance of single-crystal thanks to the help of the improved casting methods introduction and, later the introduction of processing by directional solidification that correspond to Figure 1.4.

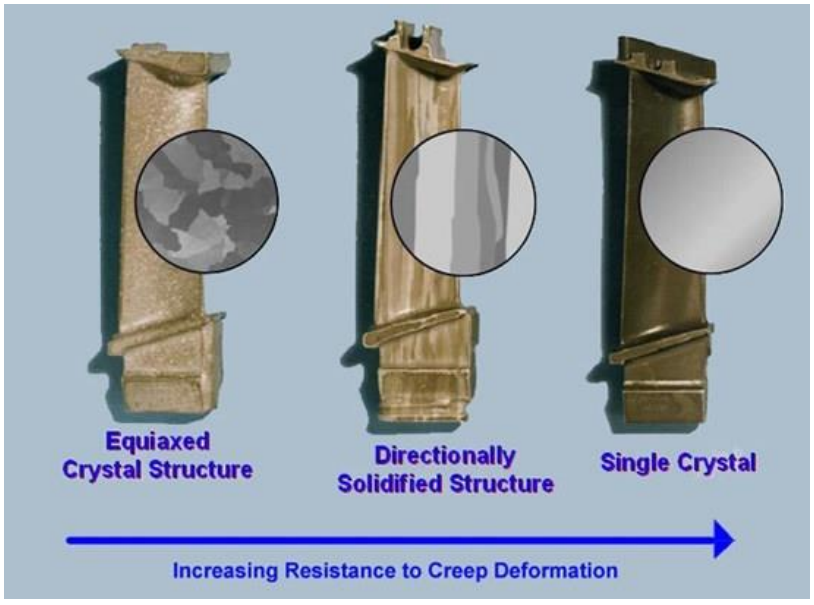

Figure 1.4 - The crystalline structure evolution [6]

1.1. Nickel superalloys

Nickel is one of the most abundant elements on earth, its atomic number is 28 and it is located in the first row of the d block of transition metals, next to iron and cobalt. The atomic weight is 59.71, which comes from 5 stable isotopes. Its crystal structure is Face-centered cubic (FCC) that correspond Figure 1.5. It is also one of the densest elements 8907 kg / m3, due to the small interactions in the atomic distance, which provides a strong adhesion by the outer d electrons [1].

1. 2. 3.

Figure 1.5 - Cubic phases in the Ni-base superalloys: 1. γ-Ni matrix, 2. γ'- Ni_3Al, 3. β-NiAl [7]

As already mentioned, Nickel presents the FCC structure and the same happens with its superalloys, distributed in the phases γ and γ ', each of them is distinguished by presenting different components in its structure. In the γ case, the elements that are included are nickel, cobalt, chromium, ruthenium, molybdenum and rhenium because these elements have an atomic radius not very different from that Nickel, in addition to almost all the cases this forms a continuous matrix phase in which other phases reside. On the other hand there is a second group of elements such as aluminum, titanium, Niobium and tantalum, which has large atomic radii and promote the formation of ordered phases in the form Ni_3(Al, Ta, Ti) known as γ ', this form is a precipitated phase, which is frequently with the γ-matrix phase. While the carbides, where the main element is coal, which occurs in a concentration of almost 2% and this is combined with reactive elements such as titanium, tantalum and hafnium, to form MC carbides and these during the operation services they can be decomposed

into other species such as $M_{36}C_6$ and M_6C, and which reside in the grain limit γ, and which are rich in chromium, molybdenum and tungsten [8].

There are other phases such as the TCP-Phases that correspond to Figure 1.5, this occurs when there is an excess of chromium, molybdenum, tungsten and rhenium, which promote the precipitation of intermetallic phases, which are rich in these elements [9]. These phases have the characteristics of large and uniform atoms packing density, a non-metallic degree, directional union and complex crystalline structure, which layers consist in a hexagonal arrangement, pentagonal and triangles stacked in a limited number of so-called Kasper coordination Polyhedral [10].

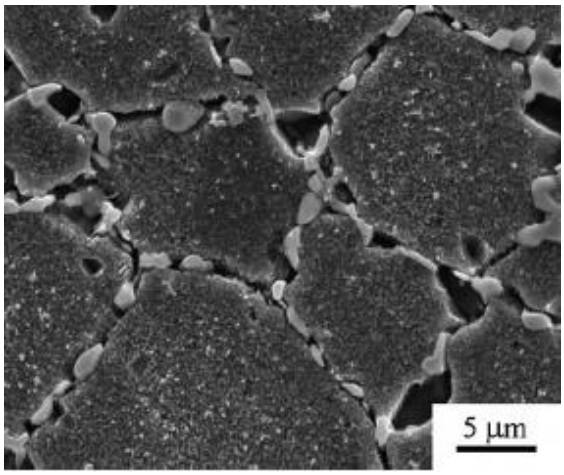

Figure 1.5 - The topologically close-packed (TCP) phases on the surface of a nickel alloy [1]

Since the 1980s, Nickel's single-crystal superalloys have evolved significantly in their chemical composition, as it improved various aspects of their properties in general. Classifying in 3 generations that is shown in the table1.1 and this is due to the Rhenium content; so SC-alloy without Rhenium (ZhS30M, CMSX-2, 3, ZhC6F, Rene 4) corresponds to the first generation; when the Rhenium content is between 2 to 3% (ZhS36, CMSX-4, Rene 5) correspond to the second generation; and with 6% of Rhenium (Rene N6, CMSX-50) correspond to the third generation [11]. There is now a fourth generation which is due to the Ruthenium and Rhenium introduction [7]. In all the aforementioned cases the Titanium concentration is reduced by the

Rhenium introduction, this is to increase the solid temperature and the volume fraction balance of γ'. The creep-strengthening effect tends to increase by the Rhenium addition. The main problem these last generations are prone to undesirable TCP-phases due to their fragility during exposure to high temperatures.

Table 1.1 - Chemical composition of Nickel alloys in different generations.

Types of	The mass percentage of elements in Ni's alloy (%)										
Ni's Alloy	Cr	Co	Mo	Re	W	Al	Ti	Ta	Nb	Hf	Ru
I generation											
ZhS30M	7	7.5	0.6	-	12	5	1.8	-	1	-	-
CMSX-2	8	4.6	0.6	-	8	5.6	1	6	-	-	-
CMSX-3	8	4.6	0.6	-	8	5.6	1	6	-	0.1	-
ZhS6F	6	10	1.3	-	12	5.5	1.2	-	1.5	1.3	-
Rene N4	9	8	2	-	6	3.7	4.2	4	0.5	-	-
II generation											
ZhS36	4	9	1	2	12	6	1	-	1.5	-	-
CMSX-4	5.6	9	0.6	3	6	5.6	1	6.5	-	0.1	-
Rene N5	7	8	2	3	5	6.2	-	7	-	0.2	-
III generation											
CMSX-10	2	3	0.4	6	5	5.7	0.2	8	0.1	0.03	-
Rene N6	4.2	12.5	1.4	5.4	6	5.75	-	7.2	-	0.15	-
IV generation											
MC-NG	4	0.2	1	4	5	5.2	1.1	5	4	0.1	4
LDSX1	3	3	2.5	6.2	2.9	6	0.25	6.5	6.2	0.1	3.5

1.2. The Nickel Superalloy of ZhS6F

In the case of this work, a nickel superalloy ZhS6F was used, which is located in the first generation that is shown in the Table 1.1. The components of this superalloy present specific functions in the structure of this superalloy. In the case of

chromium it gives a resistance to heat and hardening of solid solutions. Cobalt, molybdenum and tungsten increase the resistance to heat of a solid solution, the high content of tungsten increases the density of the alloy, but if there is an excess this promotes the formation of the TCP phases, which can have a deteriorating effect on the matrix [12-14]. Aluminum, titanium, Niobium and hafnium enter the hard γ' phase and also increase heat resistance. Vanadium hardens the solid solution, increasing the stability of the γ 'phase. The carbon prevents the formation of hot cracks for the alloy and forms carbides, which provides greater strength and durability. The greater the total content of the γ' phase in the alloy, the greater the heat resistance [16].

As previously mentioned, the γ' phase plays an important role in the hardening of Nickel superalloys, since this phase provides resistance to temperatures of up to 1200 °C. In order to provide these phases in a suitable proportion, thermal treatments must be carried out, in the ZhS6F case, hardening and aging are included. The hardening takes place at 1200-1230 °C for 3-5h, after which the quenched process is carried out where the γ' hardening phase is released. And finally the aging process takes place at 950 °C for 2h. In this process the alloy is further hardened by a slight release of γ' phase particles [17].

1.3. Oxidation and corrosion processes

The work environment of these superalloys is really severe, which leads to problems such as corrosion at high temperatures. This corrosion type is due to the oxidative acceleration of a material at high temperatures induced by a thin molten salt film deposited [18]. There are 2 types of corrosion: high temperature hot corrosion (HTHC), which involves which involves the transport of sulphur from sulphatic deposit (Na_2SO_4). The range of temperature at which this corrosion type can act is typically between 800 to 950 °C, since NiS_2 is formed (at 645 °C) and can cause degradation. The second type is Low temperature hot corrosion (LTHC), this occurs between 600 to 800 °C, its mechanism involves the formation of metal sulphates, these react with alkaline metal sulphates to form low melting points which prevent

protection oxide formation [7,19] . Analyzing both corrosion types , the one that appears in turbine blades is the HTHC and to minimize the corrosive attack goes through the section of an alloy or coating, which are capable of forming a protective oxide which is resistant to the salt film [20].

1.4.Coating types

Due to superalloys have problems of the chemical type and mechanical degradation when they operate at high temperatures, it is necessary to look for alternatives of protection, in these alternatives the coatings technology appear , since these offer the necessary protection [1] .

There are several types of thermal barriers, convenient to use [21, 22]. The most common of these coatings are the thermal barrier coating (TBC), which acts as top coat, and the bond coat in this group are located overlay coating, diffusion coatings and / or a mixture of these, corresponding to Figure 1.6.

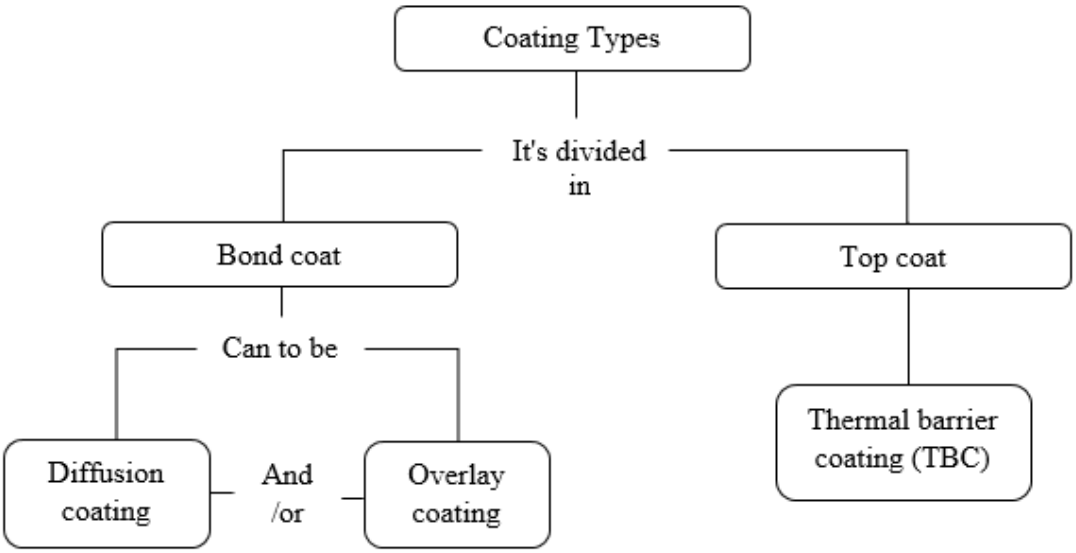

Figure 1.6 - The coating classification, according to its function when generating a TBC system.

1.4.1. Thermal Barrier Coating (TBC)

This coating type is of the ceramic type, with a main characteristic which is its low thermal conductivity. The most known case is zirconium (ZrO_2), which

compared to other oxides, its conductivity is lower [23, 24] that correspond to Figure 1.7, which surrounds 2 W/mK. It is used as top coat and is always deposited on a layer called bond coat [25, 26], due to the different coefficients of the substrate thermal expansion, overlay and top coat of the ceramic, forming a thermal stress during the thermal cycles and an eventual failure of the TBC by spallation.

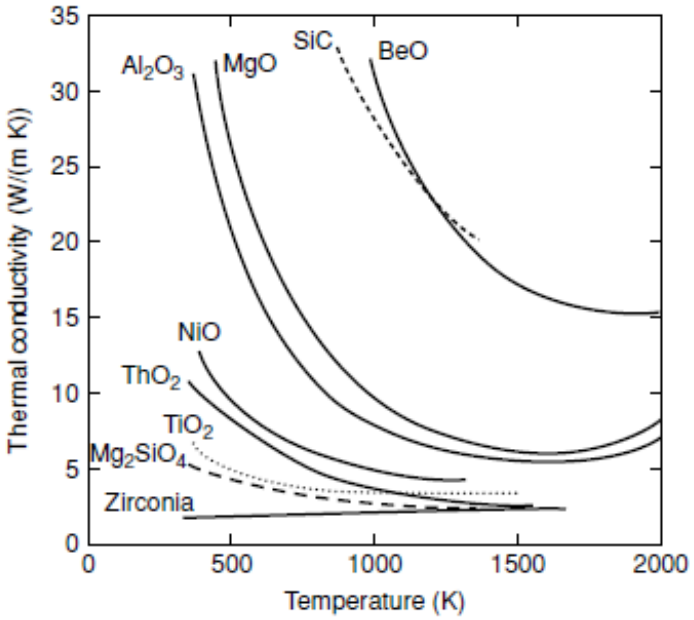

Figure 1.7- The thermal conductivity of various polycrystalline oxides as a function of temperature [23, 24]

1.4.1.1. The yttrium function in zirconium oxide

Zirconium oxide is not manufactured alone, it contains Yttrium (Y_2O_3) in the range of 6 to 11% by weight, with a composition of 7% by weight commonly used [27]. It turns out that this is the limiting composition in which the metastable (non-transformable) tetragonal phase (t'- phase) is formed when the ceramic is quenched from the cubic phase that correspond to Figure 1.8. Avoiding the transformation of the tetragonal t-phase to the monoclinic m-phase, which is associated with a 4% change in volume and leading to a poor resistance in thermal cycles and the faults appearance such as cracking and spallation at low Y_2O_3 contents. When the Y_2O_3 is combined with ZrO_2, thus forming the structure t', the term known as partially stabilized Zirconium is used and this is the TBC applications standard.

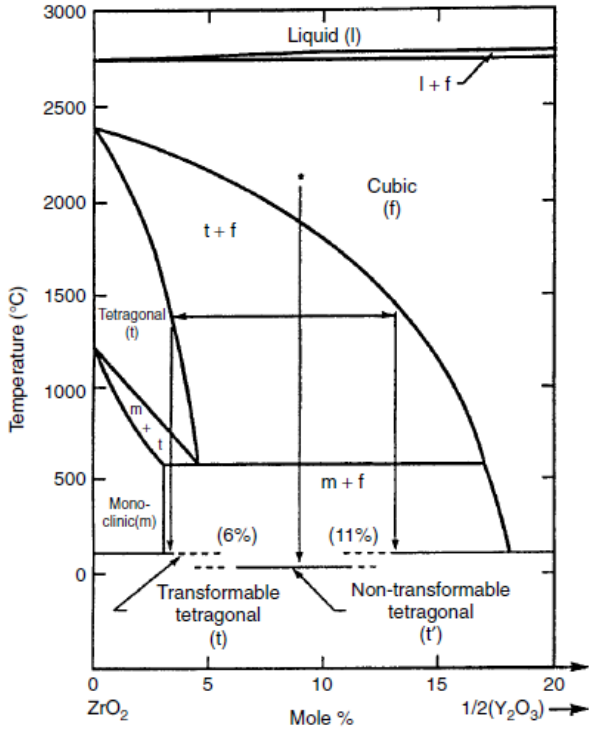

Figure 1.8 - Phase diagram for ZrO_2-Y_2O_3, showing the phase fields corresponding to the monoclinic (m), tetragonal (t) and cubic (c) phases, and the composition range for which the non-transformable tetragonal t' form is found [28].

When this coating is exposed to temperatures higher than 1200 °C, the following occurs: a partial reversion to the equilibrium phases and cubic transformation occurs with the tetragonal to monoclinic occurring in subsequent thermal cycles [28], due to the slowness of generating a reversal transformation due to the need for Y diffusion through zirconium. Another cause is the elasticity modulus increase associated with the causes of the tuning of the YSZ [29]. Both effects cause a reduction in thermal resistance.

1.4.1.2. The TBCs thermal conductivity

In a crystalline solid in general, heat transfer occurs through three mechanisms [23]:

- Electrons, which are expected to provide the best contribution at very low temperatures.

- The lattice Vibrations, which can be called at intermediate temperatures.
- Radiation, i.e. photons, which can strongly contribute to very high temperatures.

For ceramic materials are reasonably electronic insulators in general, the thermal conductivity cause at high temperatures can be given by the oxygen ion diffusion, so that the electronic contributions rest are not consider.

In the case of zirconium, its thermal conductivity tends to be reduced, due to the introduction of inhomogeneities in the glass lattice and grain structure. This is what yttrium performs which stabilizes zirconium oxide, and this reduction in conductivity increases when yttrium increases in mass percentage [30].

Other effects that must also be taken into account are the microstructural characteristics such as an intersplat boundaries and a grain column in plasma spraying (PS) and physical vapor deposition (PVD), respectively. Has a comparable effect, with the former being more effective because they are perpendicular to the direction of heat flow. Thus a coating has a low thermal conductivity when deposited by PS than by PVD. In addition, porosity has an influence on the thermal conductivity resulting from the plasma spraying process [31].

1.4.2. Overlay coatings

These coatings have the following composition MCrAlX [31, 32], where M refers to Ni or Co or a combination thereof and X is a reactive element (RE) such as Yttrium, hafnium and / or Silicon. As a consequence, its shape is metallic, and due to its nature, the composition of this coating is the substrate independent, although some interdiffusion is inevitable. Hence, its main role is to achieve the desired surface properties for given applications such as an optimum oxidation and corrosion resistance, strength and ductility mixture.

1.4.2.1. The overlay coating technological development

The first coatings of this type were developed in 1960 and were used as deposition method of the electron beam physical vapor deposition type (EB-PVD).

The first to develop were cobalt base alloys with 20 to 40% Cr, 12 to 20% Al and yttrium at levels around 0.5% [33]. So Cobalt-based coating overlays are still widely used and are recognized for their superior hot-corrosion resistance. Subsequent investigations allowed the development of coatings expanding its composition range as the addition of Si, Ta, Hf [34, 35] or precious metals such as Pt, Pd, Ru or Re [36] this was achieved with the development of technology of plasma spraying, surfacing the overlay coating based on the nickel in its composition taking into account the oxidation that the resistance to corrosion, so that an adherent Al_2O_3 oxide scale was formed during the exposure to high temperatures. The microstructure of these coating are a mixture of two β-NiAl phases and the solid solution of γ-Ni [37].

1.4.2.2. The overlay coating oxidation mechanism of Ni-based

One way to determine the oxide type formed in this coatings type (NiCrAlY) is based on the work of Petit and colleagues [38, 39], which show that the oxides formed are alumina (Al_2O_3) or Chromia (Cr_2O_3). During exposure to high temperatures, despite having more nickel in these alloys, which would be expected the Nickel oxide presence. Analyzing the ternary diagram of Ni-Cr-Al that correspond to Figure 1.9, there can be seen three scale types which are divided into group I, group II and group III, at 1000 °C, also the limits between the groups they can be affected by temperature, heat ratio and grain size.

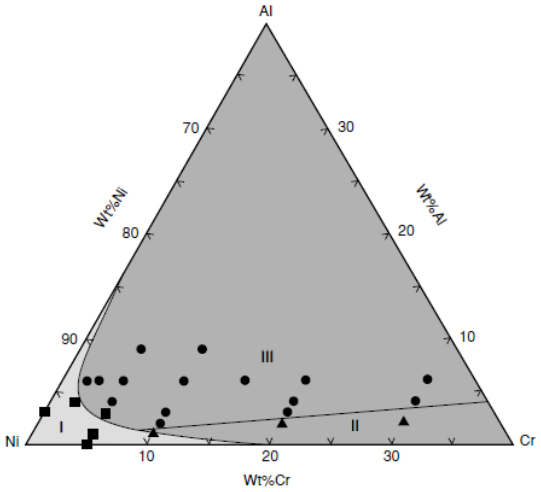

Figure 1.9 - Classification of Ni-Cr-Al alloys based on oxide and oxidation mechanism at 1000 °C [39]

The group I alloys

They are rich in nickel and have low levels of Al and Cr, characterized by a continuous external scale of NiO accompanied by a subscale of Cr_2O_3, Al_2O_3 and / or a spinel $Ni(Al, Cr)_2O_4$. Oxidation begins with spinel formation, which is quickly overcome by brittle external growth of the NiO scale; Cr_2O_3, and then Al_2O_3, are found in the lower part (interior of the substrate) due to their oxygen partial pressures low equilibrium.

The group II alloys

They are those that contain large amounts of Cr, and produce the scale of Cr_2O_3 and an internal precipitation of Al_2O_3. Initially an external scale transient mixture of NiO / $Ni(Al, Cr)_2O_4$ and sub-scale of Cr_2O_3 / Al_2O_3 is also formed, due to the greater chromium amount than the sub-scale of Cr_2O_3 replaces over time NiO/ $Ni(Al, Cr)_2O_4$ as external oxide.

The group III Alloys

They are those that contain large Al amounts, and produce the Al_2O_3 scale. Initially an external scale transient mixture of NiO/ $Ni(Al, Cr)_2O_4$ and sub-scale of Al_2O_3 is also formed inside, eventually Al_2O_3 replaces NiO/ $Ni(Al, Cr)_2O_4$ as external oxide.

1.4.2.3. The reactive element function in the overlay coating

The reactive elements [40], are added to these coatings types of to improve the scale adhesion of Al_2O_3, this happens when the quantities are small (less than 1% of weight) of Y, La, Zr or Hf or other elements of the group 3 and 4, including the lanthanides and actinides. In this elements group the one that has greater importance is the Yttrium. The amount of 0.1% by weight of Y is optimal for the growth ratio of Al_2O_3, if these levels are large at 0.5% of weight the growth ratio decreases; this is attributed to the oxides formation of reactive doping elements, such as the Ni_5Y and

Ni_2AlZr precipitated from the limit solubility to an excess of the dopant. Locating along the grain boundaries, which leads to the sublayer fragility [26].

The effects of these reactive elements according to the researches developed, are the following [1]:

- The protective pegs formation, which anchor the scale to the substrate of the metal alloy.
- Prevents vacant coalescence in the metal / scale interface by the alternative sites proportion for coalescence.
- The scale plasticity improvement.
- The cohesive energy between metal and scale is improvement.

1.4.2.4. The mechanical properties of superalloy coated with overlay coating

Due to the overlay coating deposition on the turbine components superalloy, its properties are altered [41]. In general, the coating high-temperature strength is low than the superalloys where it is placed, consequently, under load, the coating yield stress is exceeded, so the stresses in this are quickly relieved and redistributed through the section cross. In practice, it extends to a factors number to which they may be beneficial or prejudicial; as, the corrosive medium, the operating conditions, the charge nature from the crack nucleation, in fact, being the promoter and the degree to which the surface microstructure and stress state is altered. As mentioned to these coatings.

In the case of using this coating with a TBC, the resistance to thermal cycles depends on the composition of the overlay coating on which it is placed [42]. The TBC life tends to be found at the strength correlation with the resistance to the oxidation presented by the overlay, which is now acting as a bond coat [43, 44].

1.4.3. Diffusion coating

These are coatings that have aluminum as a main element in its structure, or a combination of this with nickel, chromium, silicon and always accompanied by a reactive element commonly the yttrium, where its function after being deposited on a

superalloy surface is promotes interdiffusion with the substrate, so that a layer rich in aluminum is formed on the component β-NiAl [45] surface. This coating type is commonly used as a bond coat.

1.4.3.1. Diffusion mechanism at diffusion coating

The diffusion in these coatings will depend on the aluminum activity and the aluminization temperature, leading to two processes called: Low temperature high activity (LTHA) which will allow the diffusion by the aluminum when its activity is high forming a δ-Ni2Al3 layer, this process occurs between 700 to 950 °C, which subsequently with a thermal treatment at 950-1100 °C, this δ-Ni2Al3 phase changes to β-NiAl. The other process is known as High Temperature Low Activity (HTLA), where there is a Nickel diffusion from the substrate due to the aluminum low activity forming directly the β-NiAl phase, this process occurs at high temperatures 900-1150 °C [7].

In addition there are other diffusion processes in lower concentration by the elements that make up the superalloys substrate, these cases correspond to W, Mo, Re, Ta and Ti, generating the new areas appearance and Kinkerdall porosities in the lower part of the β-NiAl phase, which is completely clean without precipitation. In the single-crystal superalloy third generation case, which are rich in Re, interdifusion promotes the formation of a secondary reaction zone (SRZ) below the interdiffusion zone (IDZ) [46,47] that correspond to Figure 1.10. This occurs due to the transformation phases discontinuity, in which a γ' matrix form contains the γ and TCPs phase needles, so the formation of SRZ causes a recrystallization of the structure γ/ γ'. Furthermore, its reaction depends on the superalloy surface preparation top priority for the coating [46].

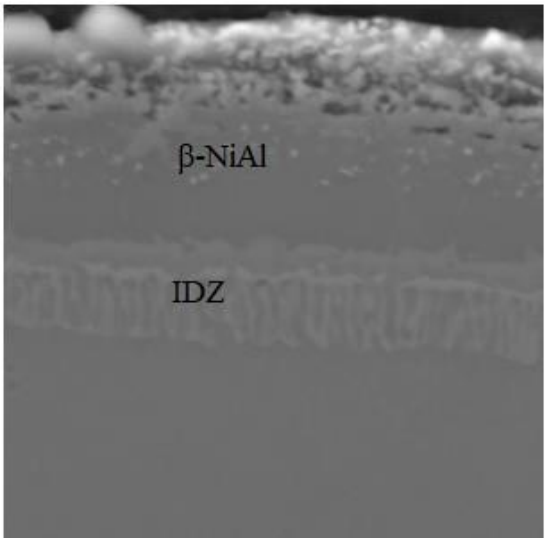

Figure 1.10 - The different zones existing after the diffusion process in the diffusion coating deposition on the first generation nickel superalloy substrate.

1.4.3.2. The alumina scale formation

After the β-NiAl phase formation, and when this is subjected to thermal cycles, α-Al_2O_3 layer is formed by the diffused aluminum loss towards the coating surface that in contact with the oxygen ion generate the oxide mentioned. This is followed by the possible oxides formation period, such as NiO, Cr_2O_3, Al_2O_3 on the surface. A layer of Cr_2O_3 is then formed under these oxides, and under which a continuous Al_2O_3 layer is developed. This process is repeated if the aluminum flow is insufficient to form a continuous scale [48].

As previously mentioned in the section 1.4.2.3 the reactive elements are added with the coating to increase the adhesion and ductility of the Al_2O_3 scale on the coating surface. An example could be the Yttrium use [49], which has a strong affinity with oxygen, generating internal oxides after the diffusion of oxygen, which are used as stakes for the alumina layer, reducing spallation during exposure to the thermal cycles.

1.5. Coating methods of obtain

The aforementioned coatings can be deposited on a nickel superalloy turbine blade, using the following equipment and processes which are involved.

1.5.1. Physical vapor deposition (PVD)

It is one of the modern processes and the most promising ways to deposit coatings [1, 50, 51]. This technology is applicable to different materials (metals, alloys, metal-ceramics) different components coatings, intended for the components work surfaces protection, tools and wear tools and erosion, environmental exposure, increase in hardness, etc.

The technology is based on the use of the following physical and chemical processes:

- The coating material evaporation in vacuum conditions.
- The vapors ionization generated by electric discharge.
- The ions movement generated in an electric or electromagnetic field to the component, in which the coating is deposited.
- Ion bombardment on the component surface, in the process that happens to clean it.
- Plasma-chemical reaction in the chemical compounds (nitrites, carbides or metal oxides) ions formation to generate these reactions in the working chamber enters a reactive gas (sulfur, methane or oxygen).
- The ions condensation on the surface with the required composition coating formation.

In the deposition of coatings by PVD in vacuum, three methods are used: Vaporization by electron beam (EB-PVD), magnetron sputtering and vaporization by electric arc. In this research work, the deposition of the types of coatings mentioned above developed by the last method.

1.5.1.1. The Vaporization by electric arc

This method consists of the following, in generating the electric arc ignition to generate a plasma between the cathode and anode from the cathode ionized vapor, which is composed of the coating material, and then depositing it on a component,

which can be of gas turbine. The process is carried out in a closed chamber under vacuum at a pressure of 10^{-3} Pa and at a given voltage.

To generate the ignition in the electric arc, the ignition electrode (anode) is necessary, this action is carried out in a short contact time of the ignition electrode with the surface of the cathode. Generating the arc burning heat between the anode and cathode in the cathode material vapors for voltages of 20-30 V and electric current of 150-300 A. The material evaporation is conducted from the spot cathode area to the arc-vacuum. A negative potential is given for the ionization and acceleration of the plasma ions to the components. If there is a high negative potential there then an ionic cleaning is carried out on the surface, after cleaning the potential value is reduced to 100 V and under these conditions the coating condensation process is carried out [52].

The characteristics of this process is the coatings obtaining that have a high resistance, strong adhesion with the substrate, scattered structures and few porosities. The peculiarity that this process presents in the diffusion coating case, is that after depositing on superalloy components, these must carry a subsequent thermal treatment, at 1000 °C in a period of 2 to 4 hours [51], the details are counted in the section 1.4.3.1.

The equipment that uses this process and used in this research work is the MAP.

1.5.1.2. The MAP-1 equipment

Equipment for the coatings many components deposition by condensation, diffusion and condensation-diffusion, among these coatings are the overlay coating, diffusion coating and TBC.

The MAP unit [51,52] that correspond to Figure 1.11, designed by the A11 Russian Institute of Aviation Materials consists of a vacuum chamber (3) accommodated in a device for generating a evaporating substances plasma flow. The equipment is made of a cylindrical cathode (1), an anode (2), an electric arc with a striking mechanism (12). By means of a special mechanism (5, 6) the cathode is

moved vertically with respect to the cooled interior of a magnetic coil, the latter fixes the arc ring ardent area on the surface of the cathode. The components (7) to be coated are arranged around the cathode in special supports, the latter rotating around their own axes. The unit is operated from above through the vacuum chamber cover.

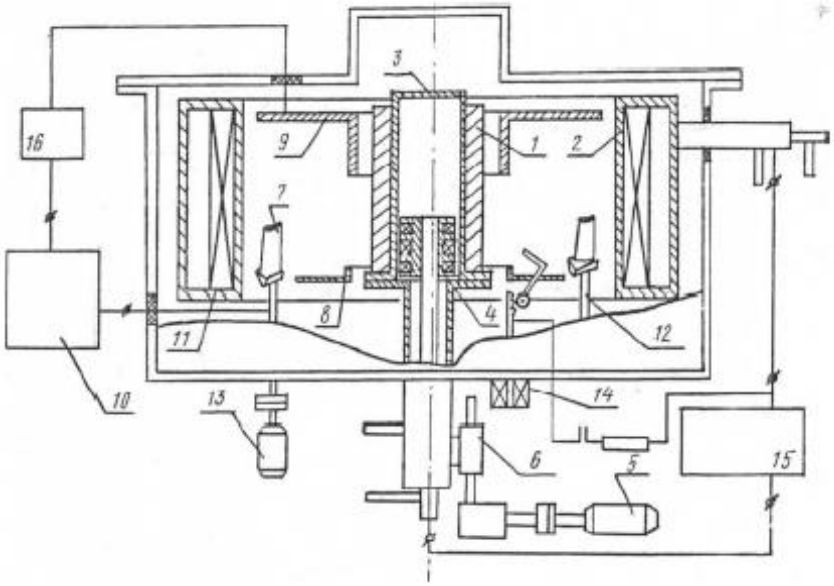

Figure 1.11 - The MAP team parts: 1, evaporable cathode; 2, anode, 3, vacuum chamber; 4, electromagnetic catch of cathode spots; 5,6, cathode vertical movement mechanism; 7, turbine blade; 8, cathode shield; 9, cachion electrode; 10, power supply of negative voltage to the blade; 11, magnetic coil; 12, electric striking mechanism; 13, unit protection from microarc striking; 14, source voltage [51,52].

1.5.2. The coatings deposition by thermal gas methods

The materials used as coatings in this deposition process type include metal, ceramic and metal-ceramic, the process consists in the bombardment to the gas turbine component surface with molten or semi-molten particles, through a gas portable jet. The material form used in this process can be wires or powders [53].

In practice there are various uses of coatings deposition by the thermal gas method such as: Electric arc spraying, vacuum spraying plasma, air spraying plasma, etc. The last mentioned method is the one that was used in this work to generate coatings.

1.5.2.1. Air Plasma Spraying

The coating material form that is used in this method is powder which has its characteristic circular shape microparticles. These in contact with the plasma are melted or semi-flooded and then deposited on the superalloy surface [1, 54-56]. The plasma consists of ionic gases, free electrons and neutral atoms, generating a hot flame close to 1000 °C. the description of this method correspond to Figure 1.12.

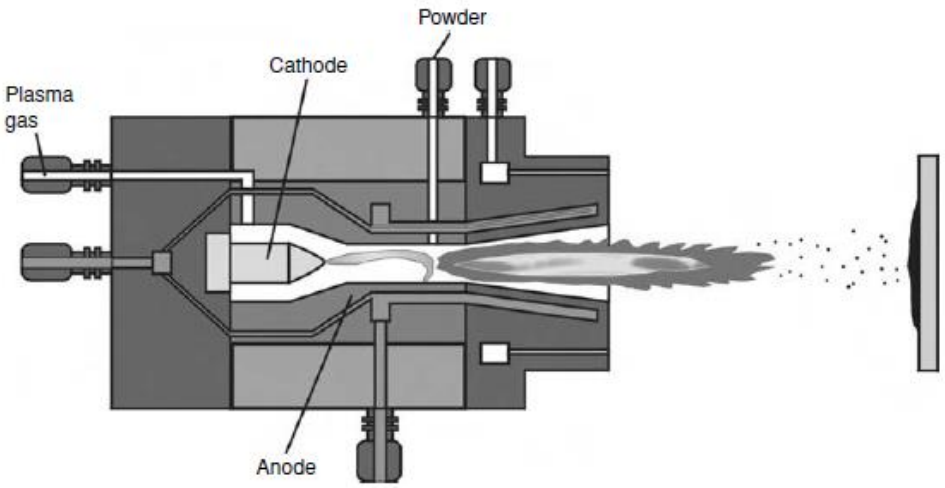

Figure 1.12- The parts that involucrate to gun at plasma spray process [1].

The gas used is typically argon or nitrogen, which flows through a tungsten cathode in an annular space housed by a copper anode cooled by water of complex shape. A high frequency electric discharge is then used to throw a direct current arc between the electrodes, which is carried by the ionized plasma causing a high temperature region in which the dust particles are introduced to be sprayed. There they are quickly melted and then propagated to the substrate to generate coating. The speed of the powder which is produced is very high almost one hundred meters per second. The plasma sprayed coatings are built particle-on-particle, producing a characteristic splat morphology. The used powders diameters the vary from 5 to 60 um, and according to their diameter they are easier to melt since the heating is more uniform around the pore and the produced coating quality is greater, since it will reduce the pores number, characteristic in this depositions type [1] .

1.6. Faults that are observed in a system TBCs

A TBC system is prone to faults, due to the action of thermal effects in the operations where they intervene or unravel, the most frequent is the delamination between the ceramic layer and the bond coat

These failures are associated with several factors, such as:

- The oxygen that enters through the ceramic top coat, forming thermally grown oxide (TGO) during the thermal cycles due to the oxidation in its interface with the bond coat, increasing the thickness with time [57, 58].

- The bond coat begins to lose aluminum with time, due to the formation of the TGO and in the interdiffusion with the substrate, in the latter the substrate provides elements not present in the coating enriching the bond coat / TGO interface and influencing life of the TBC [58].

- The action of the thermal cycles reduces the measure of the average compressive stress in the TGO [59].

- As the life of the TBC is consumed during the thermal cycle, the imperfections at or near the TGO begin to amplify. There is a difference in this characteristic due to the deposition process used, in the PVD case, the TGO is initially soft but develops undulations over time as its thickness [57], and in the case of PS when it is used, and the TGO inherits considerable roughness of the processing step and does not become rougher to any appreciable extent before failure [60].

- Incipient cracks in the form of separate nuclei in the imperfections, this growth and coalescence reduce the elastic energy strain in the system [61]. Failure occurs when the cracks one has growth to a size to support the propagation of the Buckle, usually under cooling when the ceramic layer is placed in compression [62] and the failure form that can cause this is the TBC delamination.

- The substrate different combinations lifetime, bond coat and top coat vary considerably, even using a specific method of deposition, in the ceramics case, deposition in PVD has better performance than plasma spraying with respect to strain tolerance that arise from the inherent coating microcracks processes. In the case of bond coat, the best method of deposition has not yet been defined [1].

With the aforementioned theory, the evaluation of the different systems of reverberations could be carried out and for this it is necessary to analyze methods, which will be shown next in the second part.

2. Materials and methods for coating research

The thermal barrier coatings properties study was carried out on the gas turbine engine blades obtained at the PAO "Kuznetsov" plant. The thermal protection coating on the blades was obtained in the factory in two ways: by air plasma spraying and by electric arc physical vapor deposition. The high temperature alloy ZhS6F is used for the blades manufacture as the base material. In the spraying plasma case, a four components refractory alloy bond coat of the NiCoCrAlY system was used and to create a protection layer against heat, used zirconium oxide (ZrO_2) partially stabilized with 8% Y_2O_3, while for the arc plasma physical vapor deposition case, a coatings combination of type SPD-4 and VSPD-16 was used as a bond coat and as top coat was used zirconium oxide stabilized with yttrium oxide.

The analysis in the coatings initial conditions in the powders form was only carried out for the deposition method by air plasma spray, while the base material is the same for both cases.

2.1. The blade base material

The gas turbine engine blades studied in this work were heat-resistant alloy made of type ZhS6F [15]. This alloy belongs to I generation group, due to the Rhenium non-existence in its chemical composition that is shown in the table 1.1.

Each alloy element has a specific function, as shown in section 1.2. Its characteristic structure of this alloy that correspond to Figure 2.1, γ solid solution consists based on nickel, a γ ' precipitated phase and the carbides, in the system called γ/ γ'-MC. The γ ' precipitated phase, plays an important role in the nickel-based superalloys hardening, and also has the FCC type network structure close to that of a γ solid solution. The γ' phase [16] formation the gives the alloy sufficient strength at up to 1200 °C temperatures and to achieve this, the hardening and aging processes must be carried out.

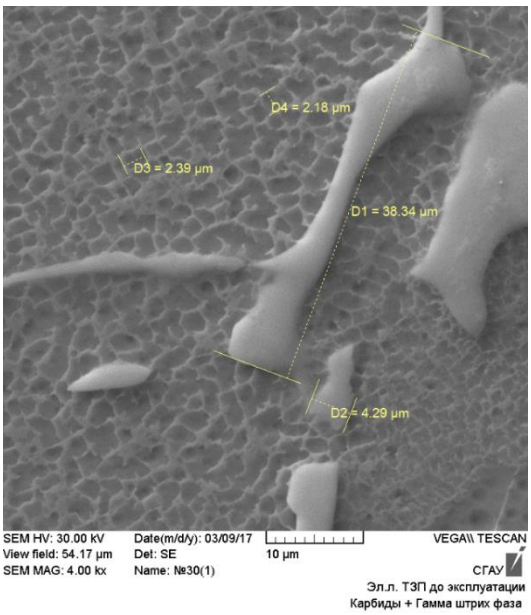

Figure 2.1 - The heat resistant nickel alloy ZhS6F structure (system γ / γ '- MC)

The carbides inclusions in the γ ' hardening phase is to withstand temperatures above 1200 °C. In ZhS6F there may be MC carbides in the "Chinese hieroglyphics" form that correspond to Figure 2.2; and M_6C, enriched with tungsten, chromium and molybdenum, the MC result after being exposed to high temperature operations. The MC carbides contain titanium and hafnium in small quantities. But when the carbides in the "Chinese characters" form are extended enough, they reduce the strength characteristics of the alloy. As a result, during the casting, this form is tried to disappear in the MC carbides [17].

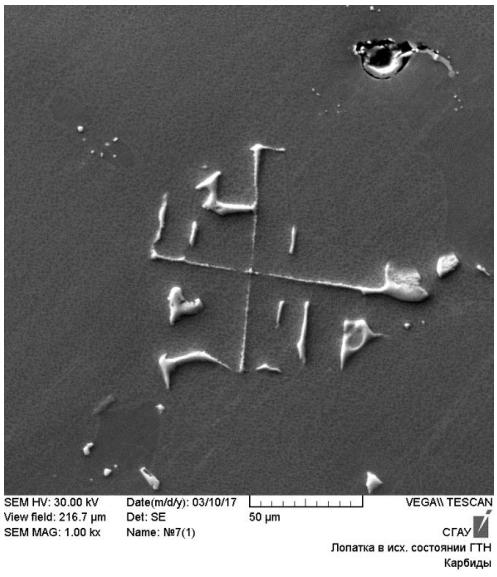

Figure 2.2 - Carbides in the "Chinese hieroglyphics" form in the heat-resistant alloy ZhS6F structure.

2.2. The bond coat material, initial powders

A four-component, the system of NiCoCrAlY heat-resistant alloy is used as a bond coat for the ceramic coating. This system implements a smooth the thermal coefficients change between the Nickel base superalloy and the ceramic top coat. The heat protection coating service life decreases with a decrease in the concentration of Al and Y in the material below a certain critical value, in which a continuous oxide coating does not form and intense corrosion begins the remaining material components high temperature. Therefore, the said heat protection coating resource in resistance terms to high temperature gas corrosion is actually determined by the coating thickness, since an increase in Al concentration above 13% and above 0.5% is not effective. The yttrium presence in low concentrations increases the metallic coating resistance [53]. If the amount of yttrium exceeds 0.5%, the coating heat resistance decreases. The reason for this is the intermetallic phase release in NiY_5 excess along the grain boundaries, which leads to the bond layer fragility, as shown in section 1.4.2.3.

For the bond coat formation on the blade surface, a heat-resistant alloy powder of the NiCoCrAlY system is used. The initial heat resistant alloy powder of NiCoCrAlY correspond to Figure 2.3, the diameters of which vary from 22.23 to 33.39 um. The powder chemical composition is shown in the Table 2.1.

Figure 2.3 -The powder appearance of NiCoCrAlY.

Table 2.1 - The powder Chemical Composition (%) of NiCoCrAlY.

substance	The mass percentage of elements (%)						
	C	O	Al	Cr	Co	Ni	Y
NiCoCrAlY	4.57	1.81	11	18.47	19.65	42.74	1.76

2.3. The top coat material, initial powders

Zirconia partially stabilized ZrO_2 + 8% Y_2O_3, consisting the tetragonal phase mainly with a small cubic and monoclinic phases amount, was used as the thermal shield ceramic layer material. The initial powder appearance that correspond to Figure 2.4, for this work three powders types were used, classified according to their diameter: less than 40 um, between 40 to 60 um and greater than 80 um. The initial powder chemical composition is shown in the Table 3.

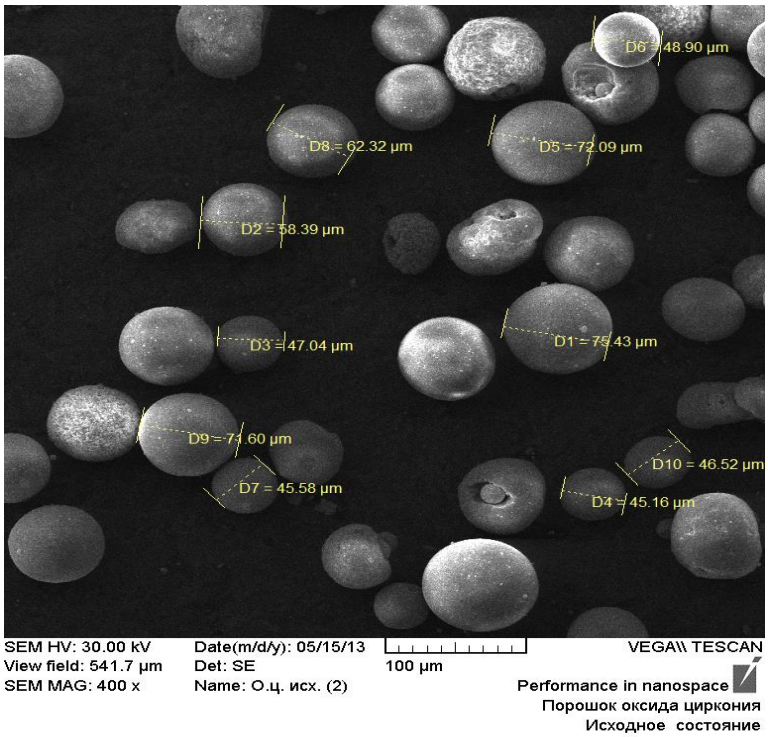

Figure 2.4 - The powder appearance of ZrO_2 + 8% Y_2O_3

Table 2.2 - The powder chemical composition (%) of ZrO_2 + 8% Y_2O_3

substance	The mass percentage of elements (%)					
	C	O	Al	Y	Zr	Hf
ZrO_2+8%Y_2O_3	8.02	33.56	2.22	6.63	48.49	1.08

In this ceramic, the m-monoclinic structure existence up to 800 °C has been established, which with an increase in temperature becomes a t-tetragonal, and at temperatures above 2200 °C in a c-cubic structure [63]. The volumetric changes that accompany the polymorphic transformation of m a t structure lead to significant internal stresses. The transformation from m to t is carried out according to the martensitic transformation mechanism, accompanied by an increase in volume from 3 to 5%. The tetragonal to monoclinic phase transformation is accompanied by an even greater volumetric expansion (4 to 6%), which can cause the ceramic cracking during cooling. Zirconium dioxide doped with Y_2O_3 oxides reduces the polymorphic transformation temperature, thus stabilizing the ZrO_2 form at high temperature, as discussed in section 1.4.1.1.

2.4. The methods that analyzing properties

The coatings give new properties to the work surface, where they are deposited thanks to a high durability and reliability combination. For this, his analysis is fundamental in the research of these coatings; there are methods such as metallographic analysis, X-ray analysis and hardening analysis [64]. Which allows to conclude if the material is suitable for specific operating conditions.

2.4.1. Metallographic Analysis

One of the main methods used in the coatings internal structure study is the metallographic method [64]. Metallographic studies provide the opportunity to implicitly evaluate the coating with the base metal adhesion strength, establish the adhesive and cohesive failure mechanisms, find cracks and discontinuities, determine the coating layers thickness, etc. This method allows to study the coating structure,

the structure and the growth of its individual components, to consider the changes in the structures during the operation.

But before carrying out this evaluation with this method, samples must be prepared in various stages that involve the processes of cutting samples, embedding with resin, sanding, polishing and engraving (if necessary) [65]. Each stage is carried out in the following way:

- The samples cutting for evaluation must have the following characteristics: they must be perpendicular to the coating; the sample area should be 1-2 cm^2, with an approximate 2.5 cm height. It is important to keep in mind that the cutting tool must move from the coating to the base metal to prevent the coating from falling off due to tensile stresses in the tool with the surface contact. The samples heating at temperatures must be avoided, it is possible to make changes in the structure. To avoid the above, refrigerants should be used when cutting the sample. The cut is made in special cutting machines with diamond circles.

- The samples already cut are coated and hardened by a polymer and a hardener mixture. This is done in cylindrical mandrels with a 10-20 mm height and a 30-40 mm diameter. With the time passage the hardening mixture is cured, when this is achieved, the sanding process is subsequently carried out.

- The sample sanding is carried out in an automatic polishing machine "LS250A" (manufactured in Italy) that correspond to Figure 2.5. When sanding, coarse-grained sandpaper is used to fine grain (abrasive marks: 180, 1400, 8000 and 1200). The sample position when sanding in the sandpaper should be parallel throughout the sanding process. When changing to another sandpaper, the section must be rotated 90° and the surface quality must be verified with an optical microscope. There should be no thicker sandpaper traces when sanding (i.e. perpendicular scratches). The sanding time in each sandpaper is 5 minutes.

Figure 2.5 - Automatic grinding and sanding machine "LS250A".

- The sanding stage remaining remains are removed by polishing. When polishing, a suspension or a paste with a dispersed abrasive is introduced into the sample surface contact area and the polishing cloth. The GOI paste use, which chromium oxide, stearin, kerosene, oleic acid and soda consists, provides the best quality to the sample. The thin samples polishing is carried out using the BUEHLER PHOENIX 4000 sample preparation system that correspond to Figure 2.6.

Figure 2.6 - Sample preparation system "BUEHLER PHOENIX 4000".

- To examine the samples, chemical etching is used to identify the TBCs microstructure and the base metal. Chemical etching occurs when a sample is immersed in a recorder. For heat-resistant nickel alloys, a the composition: CuSO 4 - 5 g, H2SO4 - 5 ml, HCl - 50 ml and H2O - 40 ml recorder.

After having made the samples preparation, they are subjected to scanning electron microscopy (scanning) allowing to increase their sizes 100 000 times in a resolution of 5-7 nm.

Thanks to the scanning electron microscope, it is possible to carry out several materials studies with coatings, such as:

- Study the turbine blade parts cracks with coatings.
- Evaluate the coatings' transverse and longitudinal sections structure nature.
- Investigate in detail the transition zone (the base metal) coating microstructure.
- Determine the quantitative the coating (by area) porosity characteristics.
- Analyze the change in the surface relief and the coating structure during wear.

2.4.2. Energy dispersive X-ray microanalysis

In conjunction with the aforementioned method in the protective coatings study, X-ray microanalysis is widely used. Thanks to this, it is possible to analyze chemical elements in a certain area, it can also be used to recognize inclusions, account for them and determine their size. The coatings chemical composition was carried out using an X-ray microanalyzer with an INCA Energy OXFORD instruments system energy dispersion. The coatings elemental analysis allows to explore the presence, content and elements distribution [66].

The metallographic and X-ray analysis was performed in a scanning electron microscope TESCAN Vega SB that correspond to Figure 2.7. The TESCAN Vega SB microscope has a tungsten cathode with thermionic emission, optically has four "Wide Field Optics" lenses that use an intermediate lens to optimize the beam shape and size. The resolution is 3.0 nm and is carried out in vacuum conditions with a 30 kV voltage.

Figure 2.7 - TESCAN Vega SB electron microscope with X-ray microanalyzer INCA

2.4.3. Hardening Analysis

In the hardening analysis [67, 68], the resulting coatings hardness was evaluated after being deposited on the turbine blade surface. To do this, the Vickers hardness evaluation method was used, which consists of subjecting the load to the sample surface with a standard load (weight) for a certain time. The load has a pyramidal diamond, which after being removed from the sample. The surface where he acted leaves a mark that correspond to Figure 2.8, this presents two diagonals, which by means of the hardness Vickers (HV) equation:

$$\mathrm{HV} = 1.854\frac{\mathrm{F}}{D^2} \qquad (2.1)$$

Where: F - applied load, Kgf;

D - the printed diagonal length,mm.

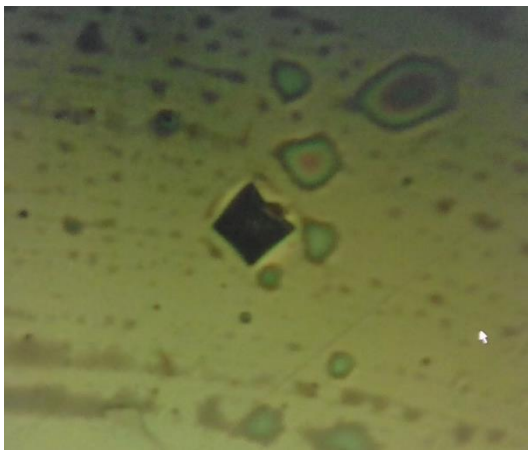

Figure 2.8 - The mark after the diamond in pyramidal form indentation on the coating.

In the coatings evaluation case, a the "DM2A" brand Vickers durometer that correspond to Figure 2.9 and the following evaluation parameters were used: a 0.025 kgf standard load was applied on the sample surface for 10 s, The resulting indentation diagonal is measured under an electron microscope, this process is repeated in a 11 tests total.

Figure 2-9: the "DM2A" brand Vickers hardness tester.

These previously mentioned methods are those with which the coatings were evaluated, involving both the deposition by air plasma spraying and arc electric physical vapor deposition processes. Showing its structure, its chemical composition and its hardness both in the evaluation of its initial state, after generating the coating and subsequently to the operation (the exploitation test).

3. Thermal barrier coatings obtained by plasma spraying

The method of obtaining by air plasma spraying is an alternative to obtain TBCs systems, capable of supporting high temperature conditions. Analyzing this method, the fundamental quality is simple in its use because the operating conditions are outdoors without the need to use a high vacuum like other processes. In this method, micro-sized powders are used as raw material, which are melting totally or partially by plasma torch means and by the impulse of this will be deposited on the sample surface or gas turbine parts consequently generating a protective coatings.

3.1. The effect of powder fractional composition on the structure and properties of the coating on model samples

For the deposition and generation of the TBC System, double layer, it was used as a bond coat to the overlay coating of NiCoCrAlY where its deposition powder diameters varied from 22.23 to 33.39 μm in diameter, while for the top coat a ceramic coating was used. The ZrO_2 + 8% Y_2O_3 classified into three different groups according to the powder diameter to be deposited, less than 40 μm, between 40 to 60 μm and greater than 80 μm. This led to the generation of three systems with different characteristics that correspond to Figure 3.1, thicknesses of different coatings that is shown in the Table 3.1. Due to this, the appropriate system type must be selected from the powder diameters used for the formation of this ceramic layer.

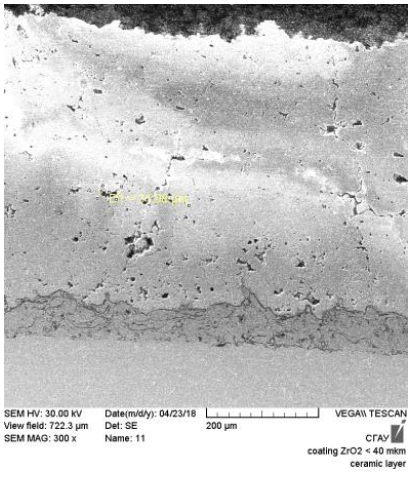

1.

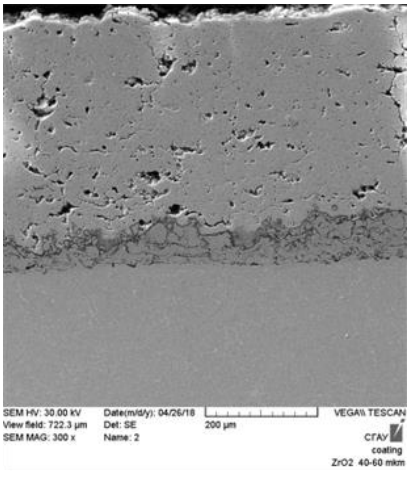

2.

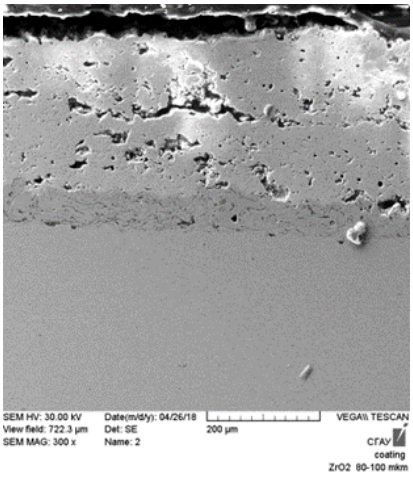

3.

Figure 3.1-The TBC systems formed and classified according to the deposited powder diameter of zirconium oxide stabilized with yttrium: 1. less at 40 μm, 2. Between 40 and 60 μm and 3. Greater than 80 μm.

Table 3.1- Thicknesses of three TBCs' systems formed

Coat	Thickness for the TBCs system, classified by powder diameter of ZrO_2 + 8% Y_2O_3 deposited (μm)		
	< 40 μm	40 - 60 μm	> 80 μm
NiCoCrAlY	78.69	73.88	61.75
ZrO_2 + 8% Y_2O_3	422.71	380.86	270.86
Total	501.4	454.74	332.61

Morphologically the upper layer structure of the three formed systems, is the porosities and cracks observation which are spread over the entire surface of the coating, this is due to one of the deposition method characteristics by air plasma spraying; since at the melting moment the powder of the coatings, they are carried out partially and totally placing one on top of the other, leaving free spaces between them until completing the coating generation on the sample surface completely. According to the observations made on the scanning electron microscope Tescan Vega SB, the porosities size are large when the ceramic powders diameter used is large, compared to the small powder diameters, generating much smaller pore diameters. The resulting ratio between deposited powders and generated powder diameters is directly proportional that correspond to Figure 3.2, while the cracks at the grain boundaries (crystallites) and in the porosities are seen in large numbers in the areas with the largest pores number that correspond to Figure 3.1.

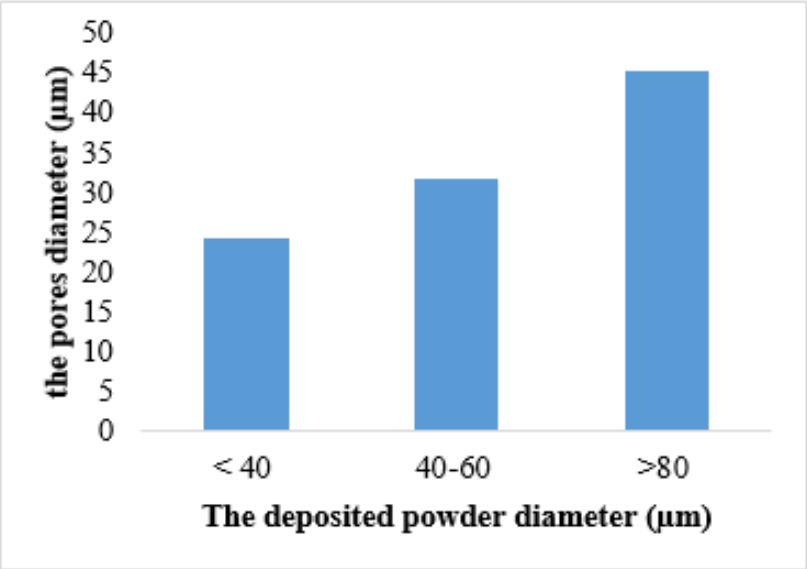

Figure 3.2 - Relation between the deposited powder diameter and the pores diameter in the top coat of zirconium oxide in tetragonal phase stabilized with yttrium oxide.

The pores number is another factor that influences the deposited powders diameters; since, these are in greater quantity when the deposited powders diameters have smaller diameters than in comparison with the powders larger diameters, which generate lower pores amount. But the porosity determined in a photographed area that correspond to Figure 3.3 and is shown in the Table 3.2by the microthoscope, for each type of TBC system, showed that in the system “<40 um" it has a lower porosity; there are greater areas of coatings without free spaces, while the porosity will increase with respect to the other powder diameters. This suggests that the porosity plays an important role in the hardness and control of the loads and thermal cycles to which these coating systems are subjected.

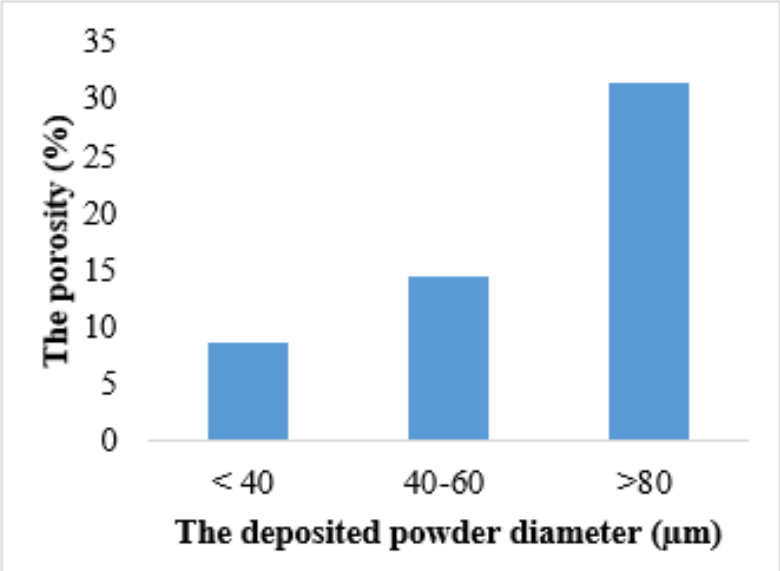

Figure 3.3 - Relation between the deposited powder diameter and the porosity in the top coat also of zirconium oxide in tetragonal phase stabilized with yttrium oxide.

Table 3.2 - The pores statistical values in the zirconium oxide layer in tetragonal phase stabilized with yttrium oxide depending on the deposited powder diameter type to generate this layer.

The powder diameter (ZrO_2 + 8% Y_2O_3)	The pore diameter, µm			The pore number			Porosity (%)
	Min.	Max.	Average	Min	Max.	Average	
<40 µm	21.47	35.58	24.25	50	64	57.25	8.57
40-60 µm	7.72	64.63	31.71	45	59	51.2	14.51
>80 µm	20.31	86.2	45.35	45	32	38.6	31.48

In the hardness analysis, each of these systems, in particular the ceramic layer, were subjected to the Vickers hardness test, for which a 0.025 Kgf. standard weight was used. The test was carried out in areas free of porosities and cracks, yielding the values shown in the Table 3.3, where it can be seen that in the ceramic system with a

lower porosity percentage, the hardness is higher compared to the others that correspond to Figures 3.4 and 3.5.

Table 3.3 - Statistical values of the indentation diagonal and hardness Vickers (HV) in the top layer for different deposited powder diameters

Parameters	The deposited powder diameter of ZrO_2 + 8% Y_2O_3 (µm)		
	< 40 µm	40-60 µm	>80 µm
D average,	8.4	11.6	14.2
D max,	8.7	11.8	14.6
D min,	8.2	11.3	13.9
HV	802.1	350.8	231.1

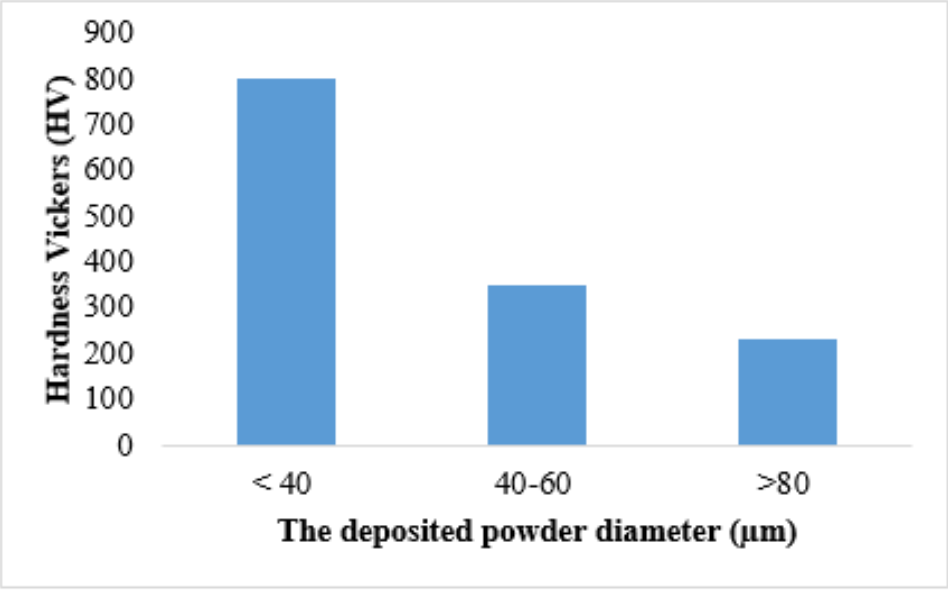

Figure 3.4 - Relation between the deposited powder diameter of zirconium oxide in tetragonal phase stabilized with yttrium oxide and the Vickers hardness (HV) evaluated in the top coat.

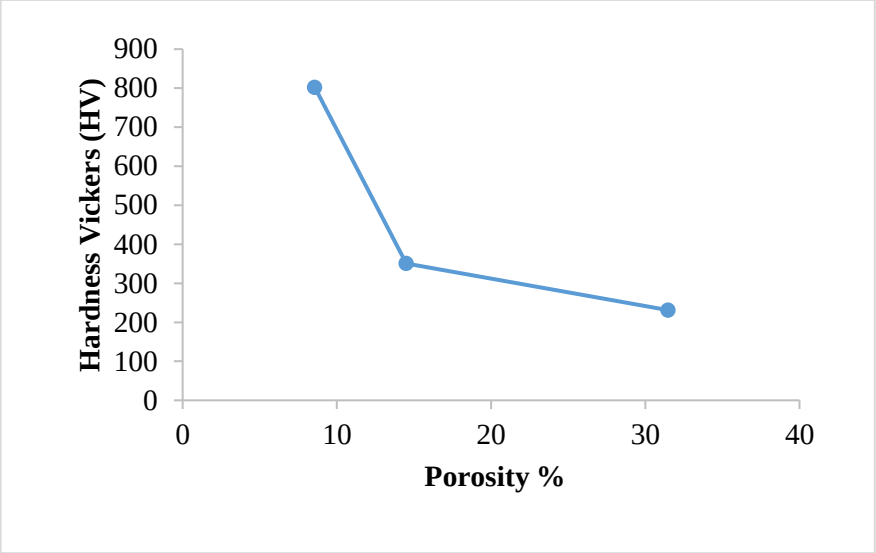

Figure 3.5 - Relation between the porosity of zirconium oxide in tetragonal phase stabilized with yttrium oxide and Vickers hardness (HV) evaluated in the top coat.

Said analyzes previously evaluated determined the feasible sample when using, which is the system formed by powder diameters less than 40 μm of zirconium oxide stabilized with yttrium oxide used as top layer in a TBC system.

3.2. Blade coating structure in the initial state

As it is well known the TBC system used in the coating formation will be of two layers, with a ZrO_2 + 8% Y_2O_3 external ceramic layer , initially formed of a diameters powder smaller than 40 μm, and a NiCoCrAlY bond coat , initially formed by powder diameters from 22.23 to 33.39 μm, using the method by air plasma spraying. This system was selected for its better hardness characteristics and lower porosities and cracks compared to the other two systems evaluated. The thicknesses of this system varied from 126 to 216 μm, this time a turbine blade was used as a Nickel alloy sample ZhS6F.

The top coat of zirconium oxide composition stabilized with yttrium oxide, has the main role of thermal insulation. The cut studies made in the ceramic layer of coating showed a structure in the layers form, and which consists of disc-shaped crystallites located along the coating surface, closed pores located in the crystallites

vertical limits region, as well as unmelted shattered particles that correspond to Figure 3.6.

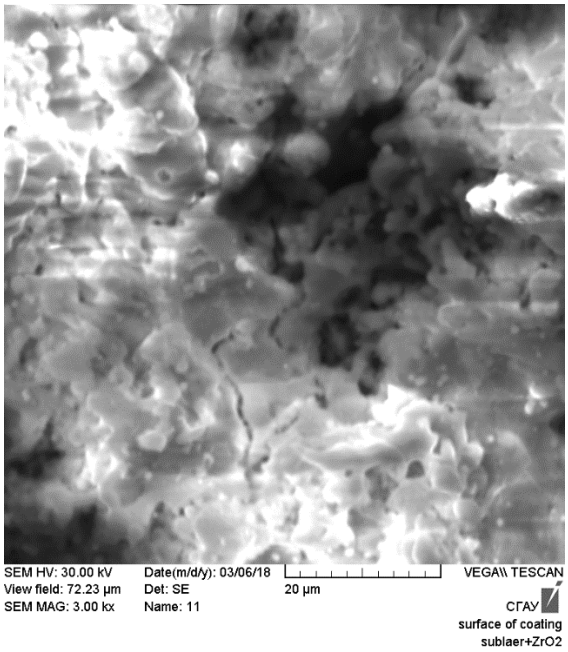

Figure 3.6 -Surface of the ceramic coating, after having used the deposition method by air plasma spraying.

The microstructure of a separate crystallite is a fused shell and a fragmented core, the melted crystallized surface of each particle has a columnar structure, the individual columns size is 50 to 70 nm that correspond to Figure 3.7.

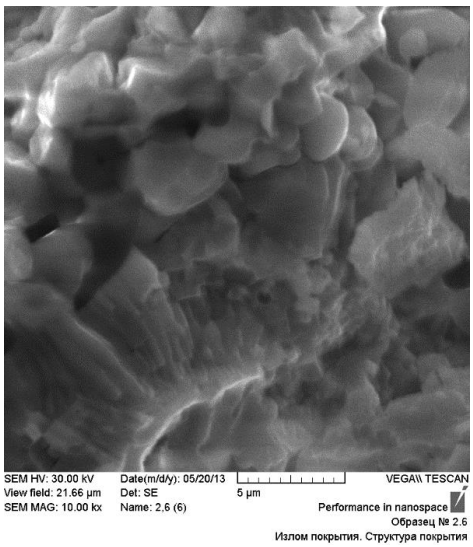

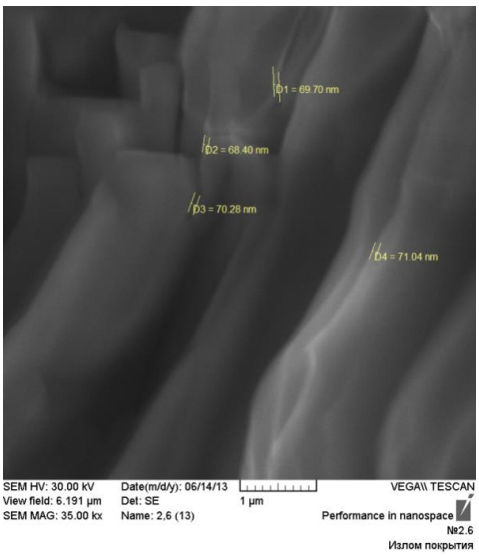

1. 2.

Figure 3.7- The microstructure of a separate crystallite in the outer ceramic layer of the TBC system in the initial state: 1. General view, 2. Thin structure.

In Figure 3.8, can see the ceramic layer structure with microcracks, which have a perpendicular and horizontal orientation with respect to the substrate where it was deposited, this determines its thermal resistance to the loads of the thermal cycles during the operation, since the beneficial orientations are perpendicular, while the horizontal ones are harmful.

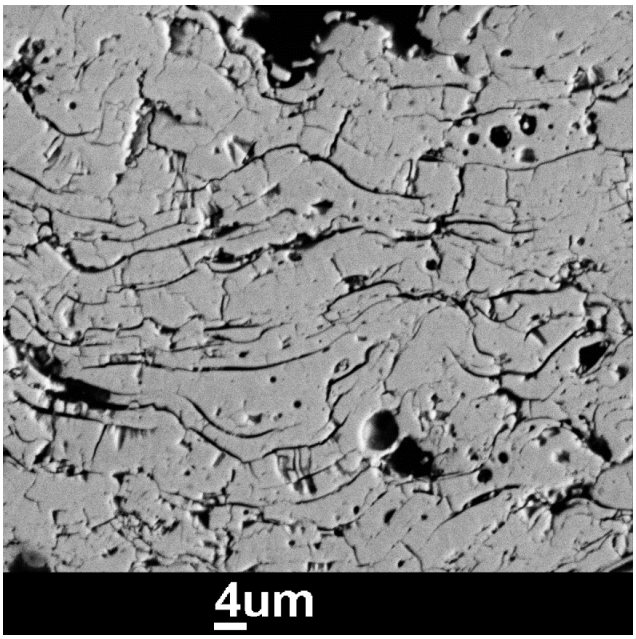

Figure 3.8 - The outer ceramic layer structure of the TBC system in the initial state.

Another characteristic that presents these ceramic coatings are their cavities and porosities in irregular shape, large and small pores that correspond to Figure 3.8. These porosities must have a certain size, since these are stress concentrators and inhibit the cracks development; therefore, there must be some porosity in ceramics to increase the permitted deformations that occur under the influence of thermal cycle loads.

To protect the base metal from oxidation, a NiCoCrAlY coating is applied to counteract the substrate release with the ceramic layer and compensate for the stresses in the heat protective coatings. Its crystalline structure is a mixture of β-NiAl and γ-Ni phases.

The bond coat structure is a layer with a large number of molten and semi-molten fragments of the material initially used (powders) that correspond to Figure 3.9.

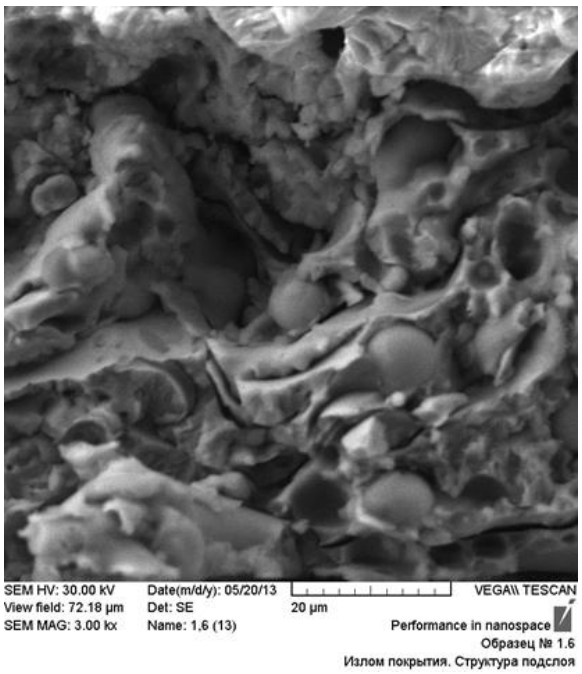

Figure 3.9 - The fracture structure of the heat-resistant inner layer of the TBC system in the initial state.

3.3. Coating structure after operation

The effect of gas flow at high temperatures on the TBC system structure can be evaluated by examining the condition of the gas turbine blades after operation. Experience shows that they are more susceptible to damage by corrosion on the blades surface in the areas: loading edge, suction side, trailing edge and pressure side that correspond to Figure 3.10. Therefore, the thermal barrier coating structure in the previously described areas should be analyzed initially, since they are of great interest.

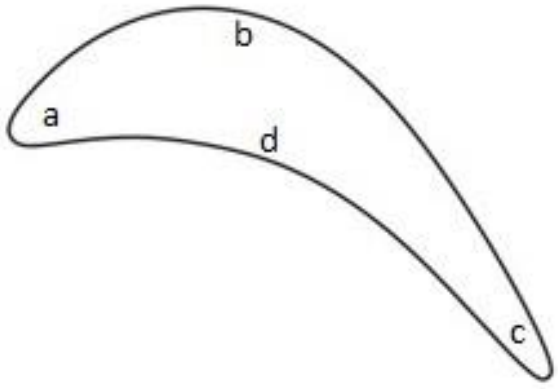

Figure 3.10 - Scheme cross section of blade: a. Leading edge, b. Suction side, c. Trailing edge, d. Pressure side

In the coating thickness analysis it can be observed that after the operation subjected to loads of thermal cycles, the coating increases in thickness due to the thermally grown oxide (TGO) formation in the bond coat limit with the top coat, due to the oxygen reaction coming from outside; which was diffused through the pores and cracks of the ceramic layer, with the aluminum present in the bond coat that correspond to Figure 3.11 besides an exhaustive comparison in each part of the blade, it is observed that the increase is in greater proportion in the pressure zone side, that compared to the rest. While in the area suction side is reduced, due to erosion effects. The average increase of the total thickness of the TBC system was 29.38% with respect to the original thickness that is shown in the Table 3.4.

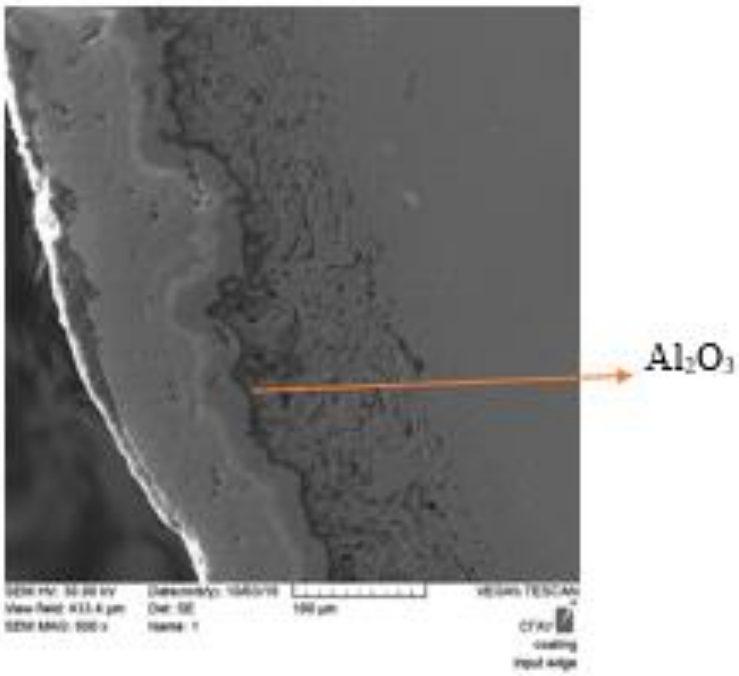

Figure 3.11 - The TBC system after operation, which shown the TGO formed

Table 3.4 - Measurements of the total thickness of the existing layers in 4 specific zones of the turbine blade made before and after of operation

Blade zones	Thickness of the total coating layer (μm)		thickness growth percentage
	Before operation	After operation	
Leading edge	125.64	230.44	83.41%
Suction side	215.86	173.27	-19.73%
Trailing edge	163.36	204.12	24.95%
Pressure side	196.76	299.92	52.43%
Average	175.41	226.94	29.38%

The ceramic layer of the TBC system, showed that after the operation, the number of pores and microcracks decreases significantly; compacting the ceramic coating pores. This indicates that the ceramic layer sintering takes place under the action of a high temperature gas stream, which are distributed in the gas turbine blade showing areas of high temperature such as loading edge and trailing edge and others of lesser such as suction side and pressure and this is shown in Table 3.5 and Figure 3.12. This leads to an increase in the coating microhardness that is shown in the Table 3.5 and, due to the porosities decrease over time under the high temperatures influence. The correspond figure 3.13 shown that the hardness is ascending of the side, loading edge and pressure side, but then it becomes trailing edge, .

In the overlay coating case of NiCoCrAlY, after being subjected to the operation, a layer of aluminum oxide of α-Al2O3 appears in the limit of this with the ceramic layer, which has characteristics of barrier against corrosion at high temperatures that with the help of the yttrium (reactive element) is anchored on the bond coat surface. This oxide is the one that is formed due to the existence of the β-NiAl phase that in contact with the oxygen generates said oxide.

Another mechanism that is presented and that is inherent in the bond coat is the interdifussion of its elements with the substrate appearing a secondary reaction zone (SRZ) under the coating. This zone reaches thicknesses of 10 to 65 μm depending on

blade evaluated and the distribution of the temperature in it, reaching an average thickness of 36.34 μm that is shown in the Table 3.5 and Figure 3.14, obtaining areas of greater thickness shown in loading edge and pressure side, while they are minors in suction side and trailing edge. This secondary reaction zone occurs when the exposure time at high temperatures is more than 100 hours. The structures that appear in the secondary reaction zone differ according to the blade locations; the needles structures appear in the loading edge, suction side and trailing edge of the blade, while in the pressure side there is a plate shape directed through the bond coat that correspond to Figure 3.15.

Table 3.5 – The temperature thickness and hardness in second reaction zone measurements at 4 specific zones of the turbine blade made after the operation.

Areas analyzed in the sample	Temperature in each part of sample (°C)	The thickness in SRZ (μm)	Hardness evaluated in the ceramic layer of TBC system (HV)
Suction side	1498	9.94	1189.70
Loading edge	1570	65.16	1578.90
Pressure side	1488	49	1863.70
Trailing edge	1530	21.27	1832.70

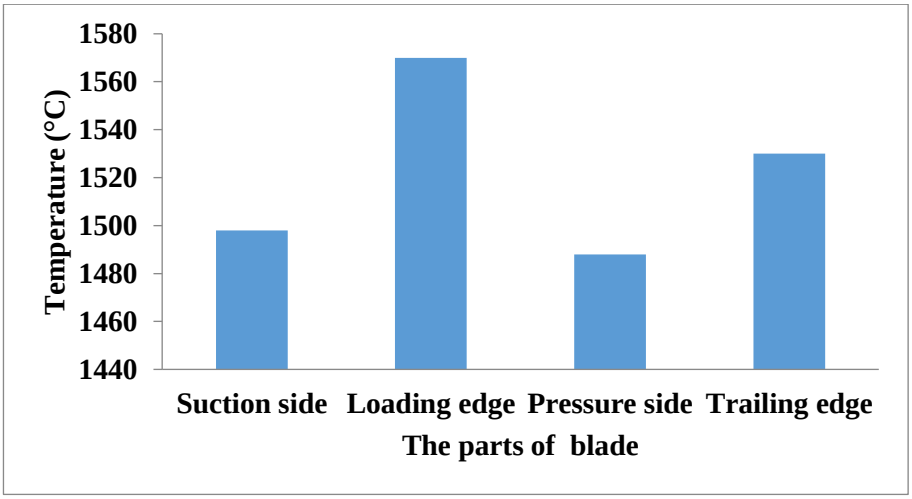

Figure 3.12 - Relation between the temperatures in each part of gas turbine blade shown in table 3-5.

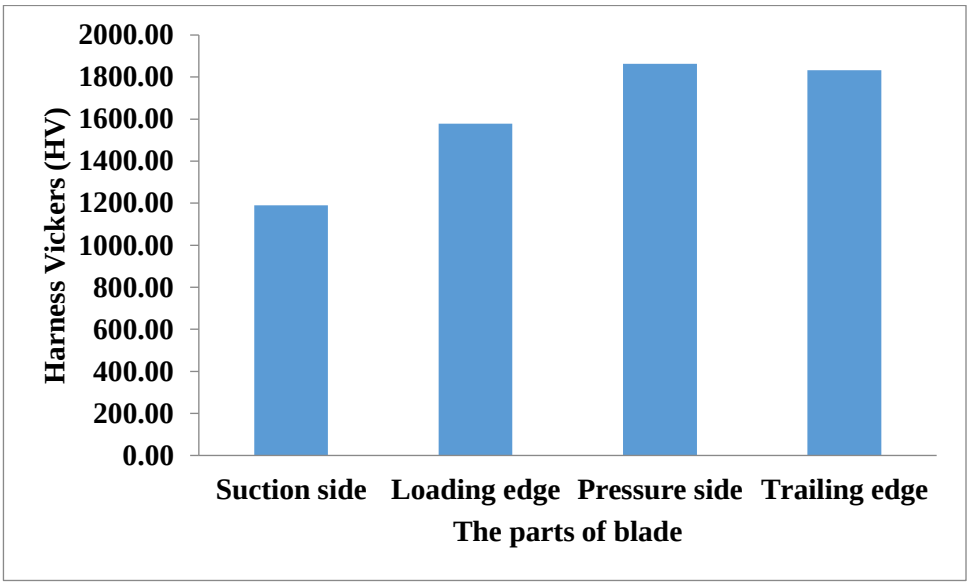

Figure 3.13 - Relation between the hardness Vickers at each part of gas turbine blade shown in table 3-5.

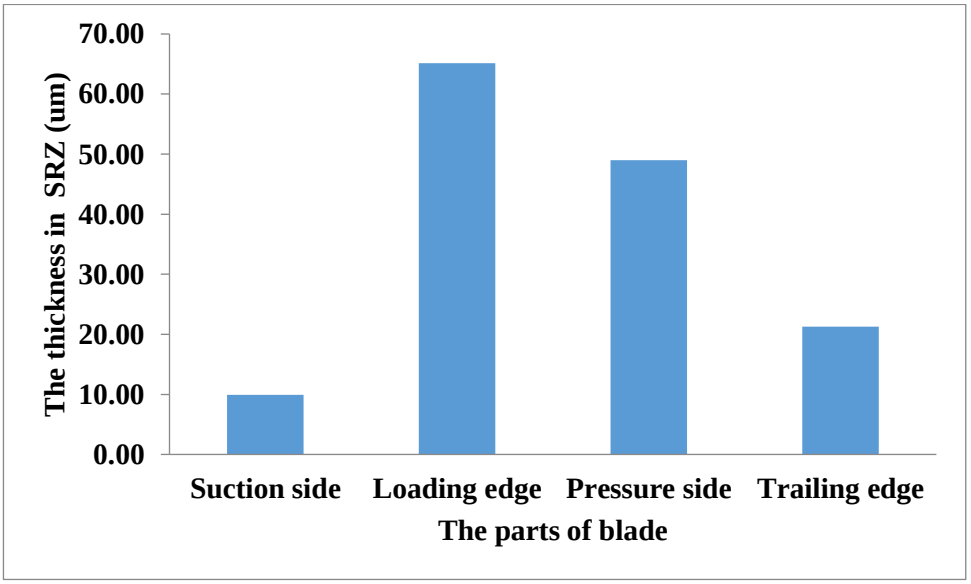

Figure 3.14 - Relation between the thicknesses in SRZ in each part of gas turbine blade shown in table 3-5.

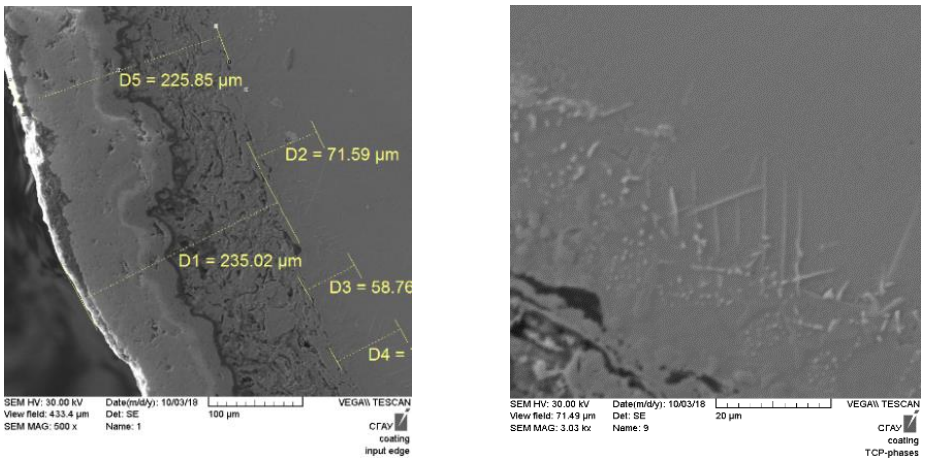

Figure 3.15 - The second zone reaction (diffusion zone) in the base metal structure on the blade working surface: 1. Leading edge, 2. Suction side, 3. Pressure side, 4. Trailing edge.

The elements' diffusion between the substrate and the bond coat increases the homogeneity between them, showing clearly in the mapping that correspond to Figure 3.16.

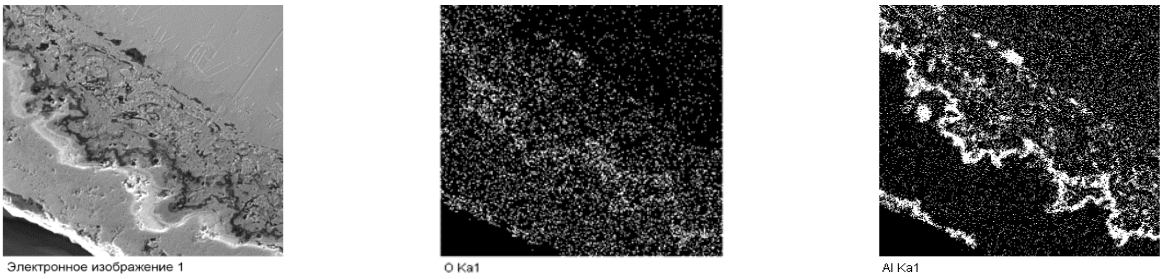

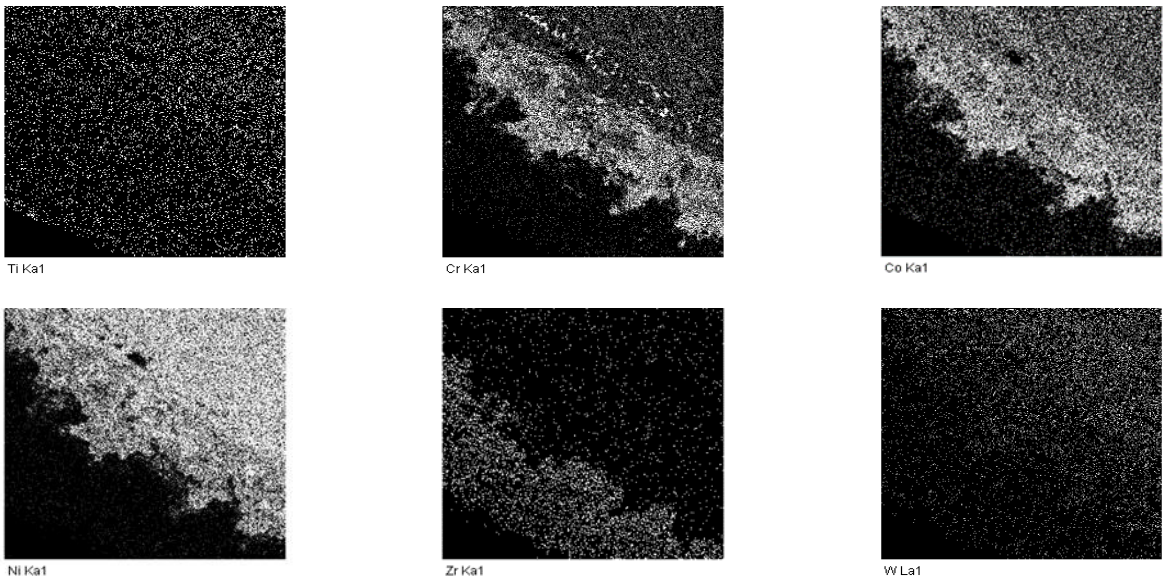

Figure 3.16 - Coating mapping after operation

The elements in the secondary reaction phase shown a greater enrichment of tungsten, chromium and carbon compared to the substrate that correspond to Figure 3.17 and is shown in the Table 3.6. These elements are grouped in a structure called topologically closed phases (TCP), which has a complex crystalline structure.

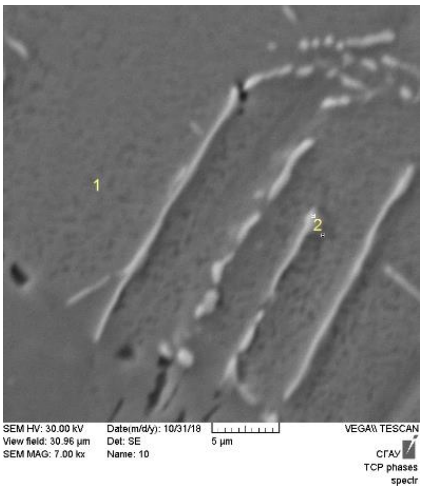

Figure 3.17 -The topologically closed packed phases

Table 3.6- The chemical composition in points 1 and 2 of Figure 3.15.

Point	The mass percentage of elements (%)										
	C	O	S	Al	Ti	V	Cr	Co	Ni	W	Total
1	7.33	-	-	5.04	1.03	0.90	5.89	12.5	57.02	10.3	100
2	9.28	0.40	0.95	2.13	0.59	1.19	9.13	10.81	37.70	27.82	100

As it is well known the carbides of the MC form, which are rich in Titanium, Thallium and Molybdenum are transformed by heat effect to structures $M_{36}C_6$ and M_6C, which are rich in Chromium, Cobalt and Tungsten. Being located in the grain limits of the γ-phase of the nickel superalloy; which forms the substrate. As the diffusion process between the substrate and the bond coat is more frequent, the carbides of the MC form, are reduced in quantity due to carbon diffusion, generating few amounts of $M_{36}C_6$ and M_6C, leading to the precipitation of topologically closed packed (TCP) phases of the μ form, which is rich in Chromium, Tungsten, Cobalt and Molybdenum.

The formation of the above-mentioned TCP phases in the substrate and under the coating with prolonged exposure to the gas flow at low temperatures reduces the structural stability of the protective coating and the heat resistance characteristics in the gas turbine engines blades.

Comparing both initial and final states of the coatings deposited by the air plasma spraying method is the diffusion process existence of both the oxygen from the outside through the cracks and pores of ZrO_2 + 8% Y_2O_3 towards the bond coat limit, generating an oxide layer of Al_2O_3 and the appearance of a second reaction zone with new TCP phases, which affect the properties of the ZhS6F alloy. For this, it was determined to perform another evaluation with the same operating conditions, using another deposition method, the arc-electric physical vapor deposition, which will be evaluated in the four part.

4. Thermal barrier coatings obtained by electric arc physical vapor deposition

There is another method for obtaining coatings called electric arc physical vapor deposition. For this process we used the MAP-1, which is an own equipment created in the Russian institute of aviation materials, for this purpose we requested support to the PAO "Kuznetsov" plant, since it had this equipment. For the TBC system, three components types were used SDP-4; which is an overlay coating of Ni metal alloy of type NiCoCrAlY, VSDP-16; which is a diffusion coating of Al alloy type AlNiY, and finally a ceramic layer of zirconium oxide stabilized with yttrium oxide (ZrO_2 + 8% Y_2O_3), the chemical composition of SDP-4 and VSDP-16 are shown in the Table 4.1. All the previously mentioned compounds have an initial form of cylinder which placed inside the MAP-1 equipment, act as a cathode that by means of erosion, magnetic electric fields and by the melting of microparticles using plasma, these are deposited on the surfaces of alloy gas turbine blades ZhS6F; which are subsequently analyzed both in the initial composition and after the operation.

Table 4.1 - The chemical composition of the components SDP-4 and VSDP-16, used in the coatings generation by the electric arc physical vapor deposition method.

Components	The mass percentage of elements (%)				
	Ni	Co	Cr	Al	Y
SDP-4	58.7	10	20	11	0.3
VSDP-16	15	-	-	83.5	1.5

4.1. Blade coating structure in the initial state

As previously mentioned, three types of components were used (SDP-4, VSDP-16 and ZrO_2 + 8% Y_2O_3), for the deposition of each component of each coating type was developed in stages. Where the first was SDP-4 coating, after being deposited on the surface of the ZhS6F sample, it was observed that the crystalline structure of the coating is similar to that of the substrate surface and in some areas the pores and cavities distinguishes the boundary between this layer with the substrate

surface, while in other parts the limit is not distinguish that correspond to Figure 4.1. The thickness obtained from coating was from 26.41 to 38.56 μm, while the percentage of existing porosities in this layer extends by 8.9% on average and the cavities and pores diameters vary from 1.74 to 11.42 μm, giving an average of 8 μm. The distance between porosities varies from 20.34 to 49.45 um giving an average of 34.1 um that is shown in the table 4.2.

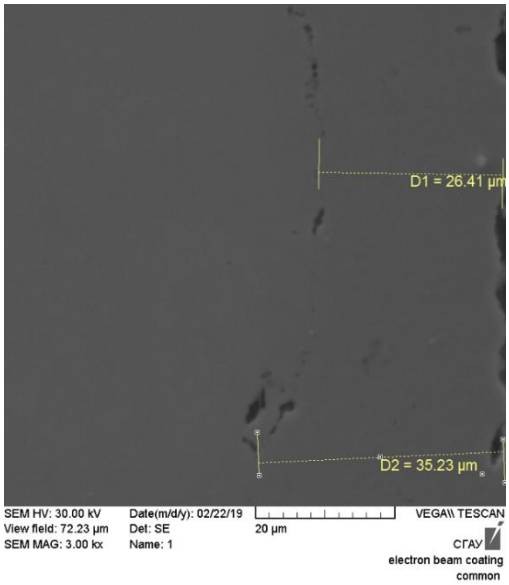

1.

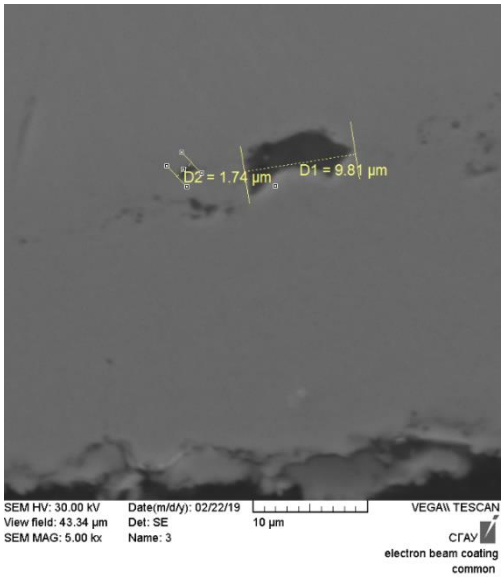

2.

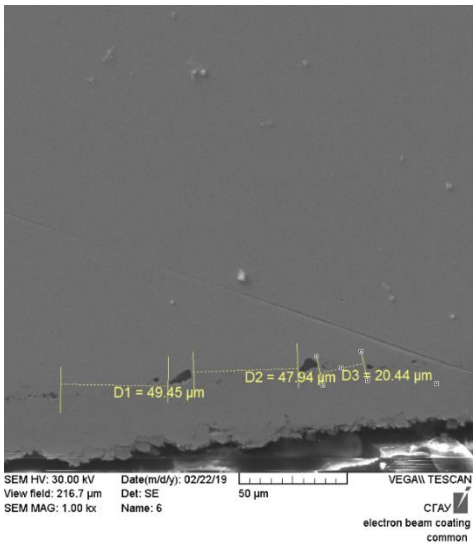

3.

Figure 4.1 - Characteristics of the SDP-4 coating deposited on the substrate ZhS6F: 1. Thickness of the coating, 2. Pore size and 3. Distance between the pores

Table 4.2 - Statistical values in the SDP-4 coating layer.

Parameters	Statistical values of the SDP-4 layer		
	Min.	Max.	Average
Thickness (µm)	26.41	38.56	31.3
Pore size (µm)	1.74	9.81	8
Porosity (%)	-	-	8.9
spaces between pores (µm)	20.34	49.45	34.1

By depositing the following VSDP-16 coating on the sample already coated by SDP-4, this produces a diffusion effect through the SDP-4 layer. This is due to the low temperature high activity (LTHA) process, allowing diffusion of the aluminum inside the SDP-4 coating and part of the ZhS6F sample to the outside of the next deposited layer of VSDP-16 forming a layer of δ- Ni_2Al_3 between the temperatures of 700 to 950 °C, which then with a heat treatment at 1000 °C this phase changes to β-NiAl. This diffusion effect not only affects aluminum, it also involves other elements which leads to the Kinkerland effect, allowing to move through vacancies, closing the pores and cavities initially shown in the SDP-4 layer.

This diffusion effect generates the interdiffusion zone and an upper layer of β-NiAl that correspond to Figure 4.2, which has incrustations of some other elements such as Iron, Cobalt and Chromium coming from the SDP-4 layer, while in the interdifussion zone appear new elements such as titanium, vanadium from the base superalloy of ZhS6F that correspond to Figure 4.3 and is shown in the Table 4.3. To check its hardness, this layer was subjected to the Vickers hardness test obtaining a result of 544.94 HV after five evaluations carried out in five different zones of the coating, compared with previous works in which they were only measured for overlay coating NiCoCrAlY (530 HV), the value obtained is greater and being a harder coating.

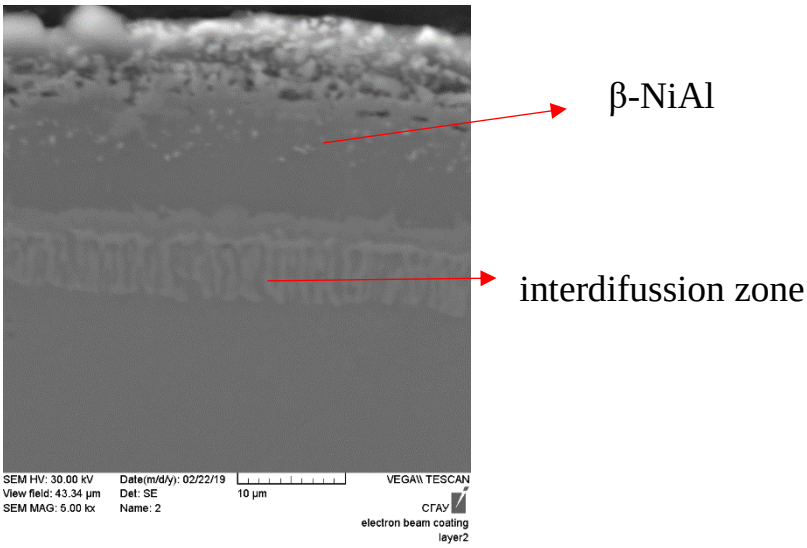

Figure 4.2 - Coating SDP-4 and VSDP-16 after the diffusion process of Aluminum.

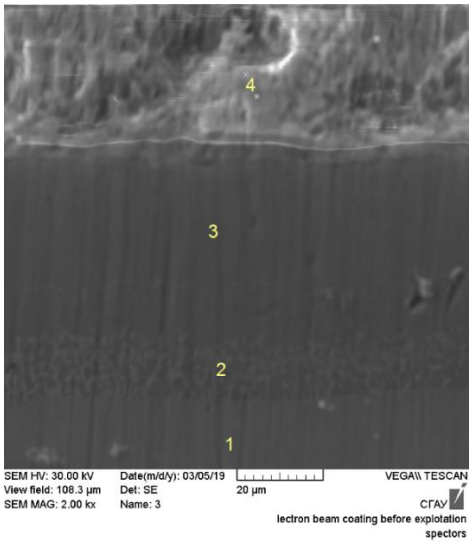

Figure 4.3 - Zones evaluated in the TBC system: 1. Substrate, 2. Interdifussion Zone, 3. Phase β-NiAl and 4. Top Coat ceramic.

Table 4.3 -The composition in each evaluation point of Figure 4.3.

Point	The mass percentage of elements (%)													
	C	O	Al	Ti	V	Cr	Fe	Co	Ni	Y	Zr	Hf	W	Total
1	6.61	0.85	6.71	1.58	0.79	4.29	-	7.58	63.01	-	-	1.97	6.6	100
2	5.48	-	11.45	0.76	0.42	20.96	0.35	9.11	45.84	-	-	-	5.63	100
3	6.31	0.92	22.66	-	-	6.63	0.25	5.71	57.45	-	0.08	-	-	100
4	20.67	27.05	-	-	-	0.22	-	-	0.33	3.54	47.27	0.93	-	100

After the deposition of these coatings, a ceramic coating is added last layer, which has the characteristics of providing thermal insulation protection, for which the zirconium oxide coating stabilized with yttrium oxide (ZrO_2 + 8% Y_2O_3) was used. Analyzing the structure of the deposited ceramic coating, it has a form of columnar grains perpendicular to the substrate where it is deposited. The widths of these grains vary from 2.94 μm to 2.31 μm (see figure 4.4). The total thickness generated for each layer deposited was 20.83 μm for SDP-4 and VSDP-16 and for ZrO_2 + 8% Y_2O_3 was 70.93 μm; It can be seen that the thickness of the bond coat layer is compacted by the diffusion effect compared to the values presented are shown in the Table 4.2.

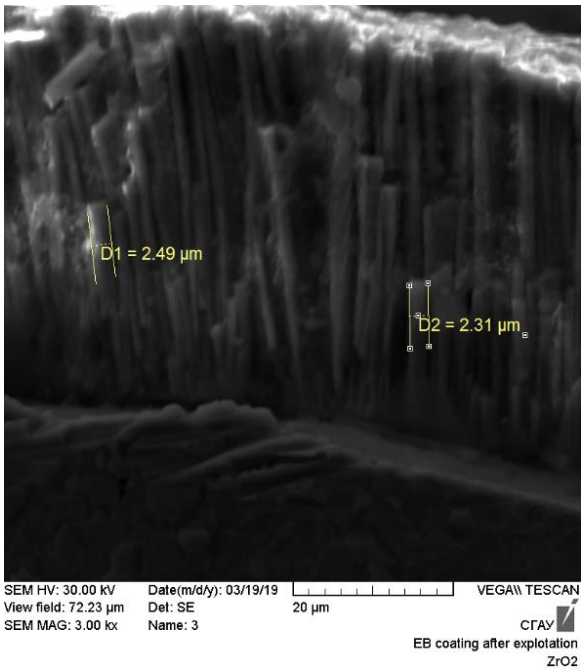

Figure 4.4 - The ceramic top coat structure of ZrO_2 + 8% Y_2O_3, after deposition by the method of arc-electric physical vapor deposition.

4.2. Coating structure after operation

In this post-operation analysis, the coating deposited on a turbine blade of ZhS6F was evaluated. The operating conditions were similar to the conditions applied to the coating obtained by the air plasma spraying method.

This is about analyzing the effect of the load on the thermal cycles that affect the coating. With respect to the ceramic coating located in the top coat, a structural resistance is observed, due to the non-change in its columnar grains structure after the

operation. Being effective at high temperatures, but not permeable because through the interplanar areas of the column grains, oxygen diffuses from the coating outer zone to the boundary of this with the enriched bond coat of the β-NiAl phase and that upon contact with this phase, the thermally grown oxide (TGO) is formed during the thermal cycles and has the α-Al_2O_3 form, increasing the total thickness of the coating by 12% on average that is shown in the Table 4.4. This layer is usually hard, stable and resistant to high temperatures; anchoring to the bond coat surface with the help of reactive elements, in this case it is yttrium, and being favorable to counteract chemical attacks at high temperatures.

Table 4.4 - Average thickness of TBC system before and after operation.

Operation	Parameters of TBC system	
	thickness total (μm)	Increase percentage (%)
before	91.76	12
after	103.61	

The generation of the TGO generates a substantial loss of Aluminum, since this gradually transforms into α-Al_2O_3, of the β-NiAl zone and the interdiffusion zone, leading to the appearance of small porosities and cavities due to the aluminum diffusion process that correspond to Figure 4.5. These cavities vary from 2.05 to 9.45 μm in size, having an average size of 4.66 μm. Its distribution and porosities is 2.9% with respect to the bond coat area. Due to this, the substrate supplies the non-existent elements to the interdiffusion zone, generating a second reactivation zone (SRZ) that correspond to Figure 4.6, that covers from 17.68 to 27.78 μm in thickness below the interdiffusion zone. It can be seen that in some areas of the sample the characteristic needles of the topologically closed packed (TCP) phase are visible, while in other areas it is not appreciable.

In the mapping analysis that correspond to Figure 4.7 in the interdiffusion zone, it was observed that the chromium is the element most concentrated in circular

granules, these are carbides of the type $M_{36}C_6$ and M_6C, due to the reaction of the primary carbides with the phase γ-Ni and the heat effect. This shows the some elements diffusion of the substrate such as Chromium and Carbon, allowing a slight increase in the composition of other elements in the substrate such as Tungsten, Cobalt and Molybdenum, precipitating in amorphous crystalline structures of complex structures called TCP phases.

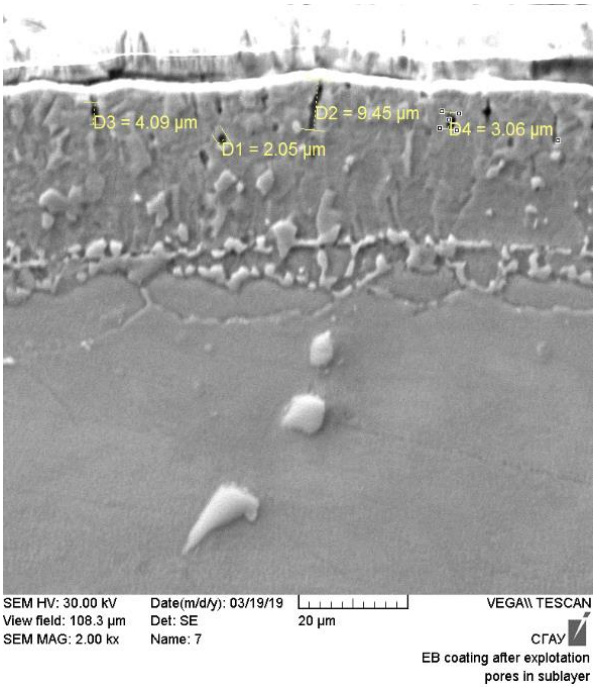

Figure 4.5 - Size of the cavities formed in the β-NiAl phase, after being the TBC system under operation.

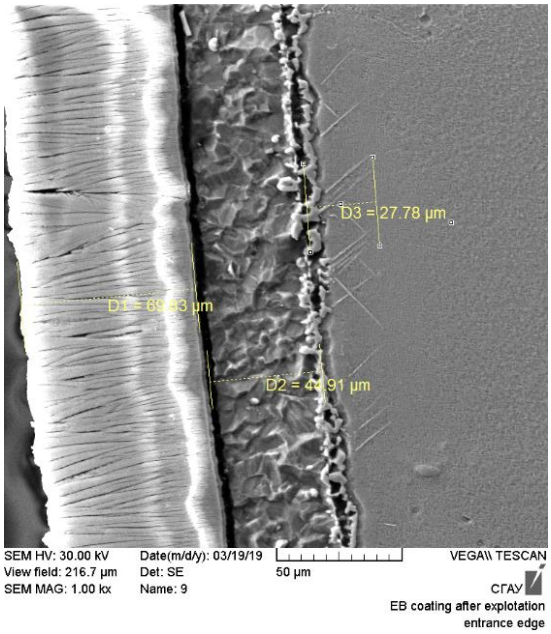

Figure 4.6 -Second reaction zone (SRZ) with TCP structures, which appears after being the TBC system to operation.

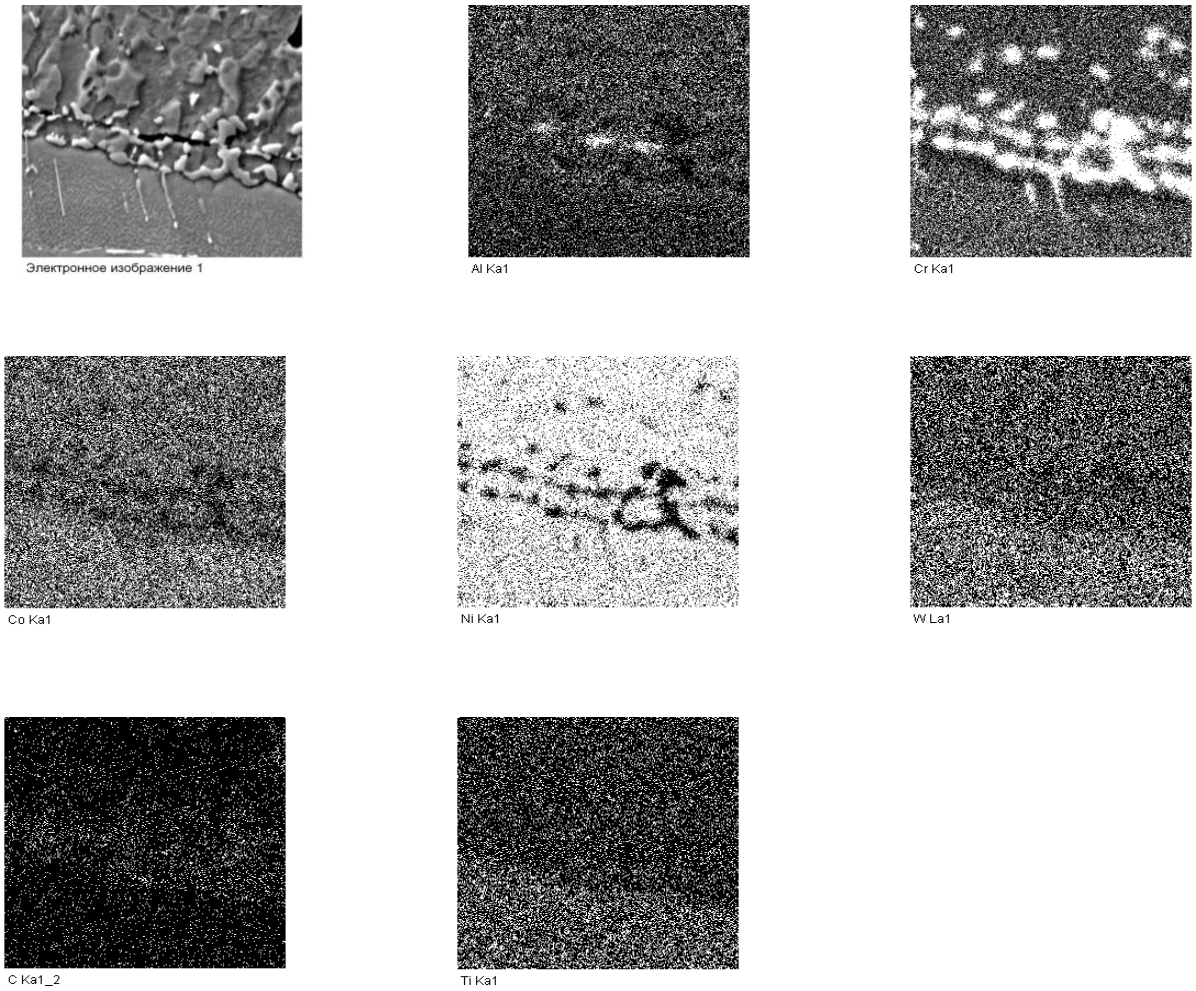

Figure 4.7- Mapping done in the second reaction zone and the interdiffusion zone.

This effect is also corroborated after the X-ray analysis of the composition of the existing components in 3 specific points (substrate, TCP and carbides in the interdiffusion zone). According to the analysis, it showed a diffusion of the elements such as Chromium and Carbon, while the elements rest did not do so in a large proportion, increasing the elements concentration such as Tungsten and Cobalt precipitating in TCP structures that correspond to Figure 4.8 and is shown in the Table 4.5.

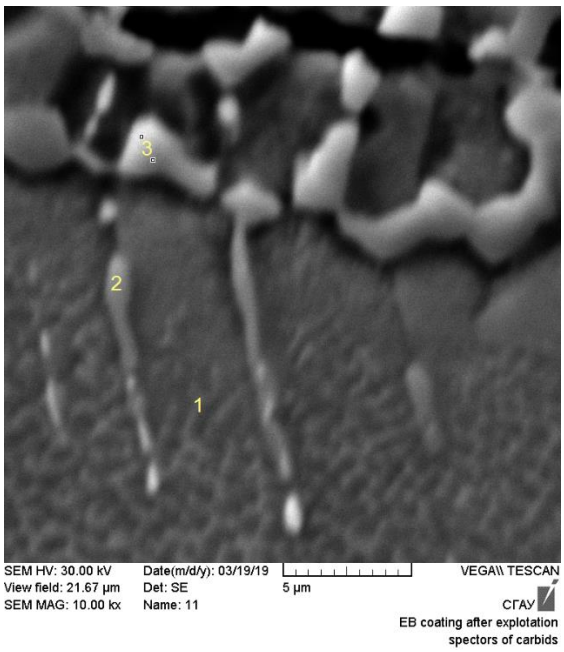

Figure 4.8 - Evaluated areas of the TBC system: 1. Substrate, 2. TCP phase and 3. Interdiffusion zone

Table 4.5: Chemical composition in each point of figure 4.8.

Point	The mass percentage of elements (%)							
	C	Al	Ti	Cr	Co	Ni	W	Total
1	8.77	5.31	1.52	7.06	10.51	56.7	10.14	100
2	14.63	3.4	1.11	25.39	5.22	39.24	11.01	100
3	20.1	4.16	0.29	26.84	4.96	37.22	6.44	100

This same x-ray analysis, which was verified throughout the entire coating, was corroborated previously, this evaluation was carried out in 6 different points. Obtaining the Carbon diffusion from the substrate internal zone towards the coating outer zone. Oxygen diffuses from the coating outer zone to the coating inner zone. The Aluminum diffusion is carried out from the substrate internal zone to the coating external zone and forming together with the oxygen Al_2O_3. The Titanium diffusion is carried out very slowly such as Tungsten, Cobalt and while Chromium is installed in zone 3 forming carbides that correspond to Figure 4.9 and is shown in the Table 4.6.

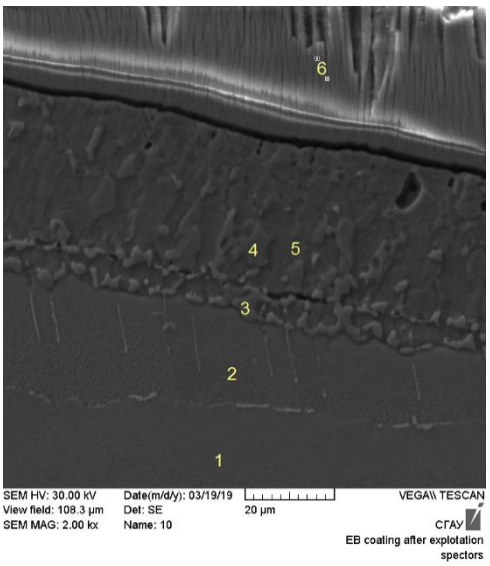

Figure 4.9 - Zones evaluated in the TBC system: 1. Substrate, 2. Second reaction zone, 3 and 4 Interdifusion zone, 5. Phase β-NiAl and 6. Top coat of ZrO_2 + 8% Y_2O_3

Table 4.6 - Chemical composition in each point of figure 4.9.

Point	The mass percentage of elements (%)										
	C	O	Al	Ti	Cr	Co	Ni	Y	Zr	W	Total
1	4.66	-	4.81	1.62	6.87	8.93	60.05	-	-	13.06	100
2	8.36	-	4.45	1.58	7.35	9.85	56.75	-	-	11.65	100
3	11.59	-	7.79	0.42	11.18	6.61	58.7	-	-	3.71	100
4	6.62	-	9.25	0.36	5.72	7.87	67.34	1.32	-	1.52	100
5	13.11	1.81	8.1	0.47	5.04	7.31	62.31	-	-	1.85	100
6	14.39	28.06	-	-	-	-	0.37	2.82	54.36	-	100

The analyzes carried out both in the initial and final state of the coating show in greater detail the diffusion mechanism of various elements existing in the substrate and coating, altering the properties, structures and / or the appearance of new phases such as TCP in the substrate and Al_2O_3 at the bond coat boundary with the top coat. These processes are in beneficial measure, since compared to the coating obtained by the deposition method by air plasma spraying the TCP phase's number; which are harmful to the substrate used of ZhS6F, is less.

CONCLUSIONS

In this part the evaluations' results of the high temperature coatings used in gas turbine blades by the deposition methods by air plasma spraying and electric arc physical vapor deposition will be discussed.

As it is well known the generation technology of coatings at high temperatures leads to the best use and sustenance of gas turbine parts, providing extra properties such as chemical protection; protecting degrading hot corrosion in hostile environments of high temperatures, extra mechanical properties that prevent wear and tear or cracking surfaces; normally product of the accumulated tensions, to be able to support the thermal cycles loads that alter the coatings internal structure.

These effects that are carried out inside the structure of these coatings, also depend on the deposition method type used. Since each one contributes different characteristics, in spite of this there are common physical-chemical phenomena such as diffusion. In addition to the coating type used, since in the air plasma spraying method the overlay coating and thermal barrier coating are involved. And by the electric arc physical vapor deposition method increases with the use of diffusion coating, this is due to the type of equipment used in this method, which is the MAP-1.

With this, the coatings systems comparison at high temperatures generated by both aforementioned methods was carried out, and thus verify their effectiveness at operating conditions of 900 to 1250 °C, acting on the alloy turbine blades ZhS6F.

The conclusions obtained are the following:

- The columnar grains structure of the ceramic topcoat of ZrO_2 + 8% Y_2O_3, is more resistant to the changes of the thermal cycles loads product of the operation, that compared to the intersplat form of the same ceramic, since the latter the structure is altered by compacting, closing and / or reducing the pores and cracks sizes. This influences the thermal insulation and the resistance of these.

- In both thermal barrier coating systems, both by the air-plasma spraying method and the electric arc physical vapor deposition, there is a diffusion of oxygen from the outside of the ceramic top coat to the limit of this with the bond coat, and

when the Oxygen comes in contact with the aluminum of the β-NiAl phase forms the α-Al2O3 or also called Thermal grown oxide (TGO).

- The bond coat formed by SDP-4 and VSDP-16 has two well-defined zones: β-NiAl phase and the interdiffusion zone, due to the diffusion mechanism of the aluminum after the VSDP-16 is deposited on the SDP-4. While the NiCoCrAlY does not show a phase separation and the coating structure is a mixture of β-NiAl and γ-Ni phases.
- The thermal barrier coating system obtained by the air plasma spraying method has a greater coating thickness than in comparison with the thermal barrier coating system obtained by the electric arc physical vapor deposition method. This is also reflected after the operation of this system on gas turbine blades of superalloy ZhS6F, because in both cases the thickness increases due to the thermal grown oxide formation but in greater proportion in the system of the first method mentioned above than compared to the second method.
- The VSDP-16 added on the SDP-4 coating, increases the Aluminum composition in the bond coat; formed by the electric arc physical vapor deposition method, to mitigate the reduction in the composition of this when it forms α-Al2O3 from the β-NiAl phase. While the bond coat of NiCoCrAlY; formed by the air plasma spraying method, the Aluminum composition is reduced due to the oxide formed under the operating conditions.
- After the operation, the topologically closed packed (TCP) phases appear in the second reaction zone (SRZ) of the substrate under thermal barrier coating systems, and are present in greater quantity in the substrates with coatings deposited by air plasma spraying that in the substrates with coatings deposited by electric arc physical vapor deposition, after the operating conditions. This suggests that the diffusion effect of the substrate components to the bond coat is in greater proportion in the first coating system described above.

After having analyzed the conclusions previously exposed, it leads to the selection of the electric arc physical vapor deposition method for the coatings at high temperatures generation, due to the shape peculiarity of the ceramic coating, giving

greater effectiveness to its characteristic of insulation thermal, the thermal grown oxide (TGO) formation for the chemical protection, the aluminum diffusion previous to the operation conditions in the bond coat ordering the structure of this and for the formation in smaller quantity of the topologically closed packed phases (TCP) in the ZhS6F superalloy substratum after being subjected to operation.

REFERENCES

1 Reed, R. C. The superalloys fundamentals and aplications [Text]/ R.C. Reed//E.: Cambridge university. – 2006. – P. 372.

2 Rolls-Royce plc. The jet engine [Text]/ Rolls-Royce plc.// Derby, UK: The Technical Publications Department, Rolls-Royce plc, - 1992. – V. 4.

3 Emoscopes. Schematic diagram of the operation of an axial flow turbojet engine [Electronic reference]/ Emoscopes// WKIMEDIA.ORG: Wikimedia server. – 2009. – URL: https://commons.wikimedia.org/wiki/File:Turbojet_operation-axial_flow-en.svg (manipulation date: 04.24.19).

4 Boyce, M. P. Advanced industrial gas turbine for power generation [Electronic reference]/ M. P. Boyce// SCIENCEDIRET.COM: Science direct journals and books. – 2012. – URL: https://www.sciencedirect.com/topics/engineering/turbine-inlet-temperature (manipulation date: 05.24.19).

5 Особенности распределения температуры по поверхности рабочих лопаток [Электроный ресурс]/ STUDFILES.NET: Stud files файловый архив студентов 1097 вузов, 2625 предметов. – 2015. – URL: https://studfiles.net/preview/22161415/page:2/ (дата обращения: 05.04.19).

6 Creep deformation of metals [Electronic reference]/ DOITPOMS.SC.UK: University of Cambridge. – 2006. – URL: https://www.doitpoms.ac.uk/tlplib/creep/printall.php (manipulation date: 04.24.19).

7 Xinghua, H. Diffusion coatings for high temperature aplications on Ni-base superalloys [Text]: Doctoral dissertation in Mechanical Engineering/ Department of Mechanical Engineering – Politecnico di Milano. – 2011. – P. 121.

8 Durand-Charre, M. The microstructure of superalloy [Text]/ M. Durand Charre// E.: Gordon and Breach science publishers. – 1997. – P. 124.

9 Reed, R.C. Characterisation and modelling of the precipitation of the sigma phase in Udimet 720 and Udimet 720Li [Text]/ R. C. Reed, M. P. Jackson and Y. S. Na / Metallurgical and Materials Transactions. – 1999. – V. 30A. – P. 521-533.

10 Sinha, A.K. Topologically close-packed structures of transition metal alloys [Text]/ A.K. Sinha// Progress in Materials Science. – 1972. – V. 15. – P. 79-185.

11 Каблов, Е.Н. Монокристаллические никеревые ренийсодержащие сплавы для турбинных лопаток ГТД [Текст]/ Е.Н. Каблов, В.Н. Толораия и Н.Г. Орехов// Труды ВИАМ. - 2002. - №7.

12 Koizumi, Y. Development of next generation Ni-base single crystal superalloys [Text]/ Y. Koizumi, T. Kobayashi, T. Yokokawa, Z. Jianxin, M. Osawa, H. Harada, Y. Aoki and M. Arai// Edited by K.A.Green, T.M. Pollock, H.Harada, T.E.Howson, R.C. Reed, J.J.Schirra and S.Walston, Superalloys 2004, TMS (The Minerals, Metals and Materials Society). – 2004. – P. 35-43.

13 Pang, H.T. A study of the effects of alloying additions on TCP phase formation in 4th generation nickel-base single-crystal superalloys [Text]/ H. T. Pang, R.A. Hobbs, H.J. Stone and C.M.F. Rae// Advanced materials research. – 2011. – V. 278. – P. 54-59.

14 Bose, S. High temperature coatings [Text]/ S. Bose // E.: Butterworth-Heinemann, 2018, Second Edition. – 416.

15 Абраимов, Н.В. Авиационное материаловедение и технология обработки металлов [Текст]: учеб. пособие для авиационных вузов/Н.В. Абраимов, Ю.С. Елисеев, В.В. Крымов. — М.: Высшая школа, 1998. - 444 с.

16 Химушин, Ф.Ф. Жаропрочные стали и сплавы [Текст]/Ф.Ф. Химушин. – М.: Металлургия, 1969, 2-е изд. – 752 с.

17 Кишкин, С. Т. Литейные жаропрочные сплавы на никелевой основе [Текст]/С.Т. Кишкин, Г.Б. Мтроганов, А.В. Логунов. - М.: Машиностроение, 1987. —116 с.

18 Neumeier, S. Lattice misfit of high refractory ruthenium containing nickel-base superalloys [Text]/ S. Neumeier, J.Ang, R.A. Hobbs, C.M.F.Rae and H.J.Stone// Adv. Mater. Resear. S. Neumerier in conference EuroSuperalloys 2010. – 2010. – V. 278. – P. 60-65.

19 Pomeroy, M.J. Coatings for gas turbine materials and long term stability issues [Text]/ M.J. Pomeroy// Mater. Des. – 2005. – V. 26. – P. 223-231.

20 Caron, P. Evolution of Ni – based superalloys for single crystal gas turbine blade aplications [Text]/ P. Caron and T. Khan// Aerospace science technology. – 1999. – V. 3. – P. 513-523.

21 Wood, J. H. Protective coatings, in C. T. Sims, N. S. Stoloff and W. C. Hagel [Text]/ J. H. Wood and E. Goldman// eds, Superalloys II (New York: John Wiley and Sons). – 1987. – P. 359–384.

22 Nicholls, J. R. Advances in coating design for high performance gas turbines [Text]/ J. R. Nicholls// MRS Bulletin. – 2003. – V. 28. – P. 659–670.

23 Clarke, D. R. Materials selection guidelines for low thermal conductivity thermal barrier coatings [Text]/ D. R. Clarke// Surface and Coatings Technology. – 2003. – V. 163–164. – P. 67–74.

24 Kingery, W.D. Thermal conductivity: temperature dependence of conductivity for single-phase ceramics [Text]/ W. D. Kingery// Journal of the American Ceramic Society. – 1955. – V. 38. – P. 251-255.

25 Pint, B. A. Substrate and bond coat compositions: factors affecting alumina scale adhesion [Text]/ B. A. Pint, I. G. Wright, W.Y. Lee, Y. Zhang, K. Prussner and K.B. Alexander// Materials Science and Engineering. – 1998. – V. A245. – P. 201–211.

26 Wang, J. S. Effects of strain cycling on buckling, cracking and spalling of a thermally grown alumina on a nickel-based bond coat [Text]/ J. S. Wang and A. G. Evans// Acta Materialia. – 1999. – V. 47. – P. 699–710.

27 Clarke, D. R. Materials design for the next generation of thermal barrier coatings [Text]/ D. R. Clarke and C. G. Levi// Annual Review of Materials Research. – 2003. – V. 33. – P. 383–417.

28 Miller, R. A. Phase stability in plasma-sprayed partially stabilised zirconia-yttria, in A. H. Heuer and L.W. Hobbs [Text]/ R. A. Miller, J. L. Smialek and R. G. Garlik// eds, Science and Technology of Zirconia, Advances in Ceramics (Columbus, OH: American Ceramic Society, 1981). – 1981. – V. 3. – P. 241–253.

29 Thompson, J. A. The effect of heat treatment on the stiffness of zirconia top coats in plasma-sprayed TBCs [Text]/ J. A. Thompson and T.W. Clyne// Acta Materiala. – 2001. – V. 49. – P. 1565–1575.

30 Nicholls, J. R. Methods to reduce the thermal conductivity of EB-PVD TBCs [Text]/ J. R. Nicholls, K. J. Lawson, A. Johnstone and D. S. Rickerby// Surface and Coatings Technology. – 2002. – V. 151–152. – P. 383–391.

31 Golosnoy, I.O. An analytical model for simulation of heat flow in plasma-sprayed thermal barrier coatings [Text]/ I.O. Golosnoy, S. A. Tsipas and T.W. Clyne// Journal of Thermal Spray Technology. – 2005. – V. 14. – P. 205–214.

32 Nicholl, A. R. Future developments in plasma spray coating [Text]/ A. R. Nicholl, H. Gruner, G. Wuest and S. Keller// Materials Science and Technology. – 1986. – V. 2. – P. 214–219.

33 Nicholl, A. R. Oxidation and high temperature corrosion behaviour of modified MCrAlY cast materials, in R. H. Bricknell, W.B. Kent, M. Gell, C.S. Kortovich and J.F. Radavich [Text]/ A. R. Nicholl and G. Wahl// eds, Superalloys 1984 (Warrendale, PA: The Metallurgical Society of AIME). – 1984. – P. 805-814.

34 Gupta, D. K. A silicon and hafnium modified plasma sprayed MCrAlY coating for single crystal superalloys, in R. H. Bricknell, W.B. Kent, M. Gell, C. S. Kortovich and J. F. Radavich [Text]/ D. K. Gupta and D. S. Duvall// eds, Superalloys 1984 (Warrendale, PA: The Metallurgical Society of AIME). – 1984. – P. 711–720.

35 Taylor, T. A. Development of alloyed and dispersion-strengthened MCrAlY Coatings [Text]/ T. A. Taylor and D. F. Bettridge// Surface and Coatings Technology. – 1996. – V. 86-87. – P. 9–14.

36 Czech, N. Optimisation of MCrAlY-type coatings for single crystal and conventional cast gas turbine blades, in J. Nicholls and D. Rickerby [Text]/ N. Czech and W. Stamm// eds, High Temperature Surface Engineering (London: The Institute of Materials). – 2000. – P. 61–65.

37 Archer, D. R. G. R. Modelling of phase equilibria in MCrAlY coating systems [Text]/ D. R. G. Archer, R. Munoz-Arroyo, L. Singheiser and W. J. Quadakkers// Surface and Coatings Technology. – 2004. – V. 187. – P. 272–283.

38 Pettit, F. S. Oxidation mechanisms of nickel-aluminium alloys at temperatures between 900°C and 1300°C [Text]/ F. S. Pettit// Transactions AIME. – 1967. – V. 239. – P. 1297–1305.

39 Giggins, C. S. Oxidation of Ni-Cr-Al alloys between 1000°C and 1200°C [Text]/ C. S. Giggins and F. S. Pettit// Journal of the Electrochemical Society. – 1971. – V. 118. – P. 1782–1790.

40 Whittle, D. P. Improvements in high-temperature oxidation resistance by additions of reactive elements or oxide dispersions [Text]/ D. P. Whittle and J. Stringer// Philosophical Transactions of the Royal Society of London. – 1980. – V. 295A. – P. 309–329.

41 Rhys-Jones, T.N. The influence of surface coatings on the fatigue behaviour of aeroengine materials [Text]/ T.N. Rhys-Jones and T. P. Cunningham// Surface and Coatings Technology. – 1990. – V. 42. – P. 13–19.

42 Brindley, W.J. Thermal barrier coating life and isothermal oxidation of low-pressure plasma-sprayed bond coat alloys [Text]/ W. J. Brindley and R. A. Miller// Surface and coatings technology. – 1990. – V. 43/44. – P. 446-457.

43 Stecura, S. Effects of yttrium, aluminum and chromium concentrations in bond coatings on the performance of zirconia-yttria thermal barriers [Text]/ S. Stecura // Thin Solid Films. – 1980. – V. 73. – P. 481–489.

44 Stecura, S. Two-layer thermal barrier coatings i: Effects of composition and temperature on oxidation behaviour and failure [Text]/ S. Stecura // Thin Solid Films. – 1989. – V. 182. – P. 121–139.

45 Goward, G.W. Mechanisms of formation of diffusion aluminide coatings on nickel-base superalloys [Text]/ G.W. Goward and D. H. Boone // Oxidation of Metals. – 1971 – V. 3. – P. 475–495.

46 Walston, W. S. A new type of microstructural instability in superalloys – SRZ, in R.D. Kissinger, D. J. Deye, D. L. Anton et al. [Text]/ W. S. Walston, J. C. Schaeffer and W. H. Murphy// eds, Superalloys 1996 (Warrendale, PA: The Minerals, Metals and Materials Society (TMS)). – 1996. – P. 9–18.

47 Lavigne, O. Relationships between microstructural instabilities and mechanical behaviour in new generation nickel-based single crystal superalloys, in K. A. Green, T. M. Pollock, H. Harada et al. [Text]/ O. Lavigne, C. Ramusat, S. Drawin, P. Caron, D. Boivin and J.-L. Pouchou// eds, Superalloys 2004 (Warrendale, PA: The Minerals, Metals and Materials Society (TMS)). – 2004. – P. 667–675.

48 Warnes, B. M. Clean diffusion coatings by chemical vapour Deposition [Text]/ B. M. Warnes and D. C. Punola// Surface Coatings Technology. – 1997. – V. 94–95. – P. 1–6.

49 Pint, B. A. Experimental observations in support of the dynamic-segregation theory to explain the reactive-element effect [Text]/ B. A. Pint// Oxidation of Metals. – 1996. – V. 45. – P. 1-38.

50 Boone, D. H. Physical vapour deposition processes [Text]/ D. H. Boone// Materials Science and Technology. – 1986. – V. 2. – P. 220–224.

51 Tamarin, Y. Protective coatings for turbine blades [Text]/ Y. Tamarin// E.: ASM International, 2002, First edition. – 247.

52 Мубояджян, С. А. Промышленная установка МАП-1 для нанесения защитных покрытий различного назнечения [Текст]// С. А. Мубояджян и С. А. Будиновский // Труды ВИАМ. - 1995. - № 7-8.

53 Пат. 2260071 Российская Федерация, МПК7С23С4/04, С23С4/12. Способ нанесения теплозащитного эрозионно-стойкого покрытия [Текст]// Балдаев Л.Х. - №2004128749/02; заявл. 30.09.2004; Опубл. 10.09.2005.

54 Барвинок, В.А. Определение остаточных напряжений в плазменных покрытиях, нанесенных на внутреннюю поверхность кольца [Текст]/В.А. Барвинок, В.И. Богданович, Ф.И. Китаев//Сварочное производство. - 1981. - №3. - С.32-36.

55 Барвинок, В. А. Управление свойствами теплозащитных плазменных покрытий деталей ГТД [Текст]/В. А. Барвинок, В. И. Богданович, И. А. Докукина, В. М. Карасёв//Вестник Самарского государственного аэрокосмического университета. - 2012. - №3. С. 44-51.

56 Будиновский, С.А. Разработка теплозащитных покрытий для рабочих и сопловых лопаток турбины из жаропрочных и интерметаллидных сплавов [Текст]/С.А. Будиновский, А. А. Смирнов, П. В. Матвеев, Д. А. Чубаров//Труды ВИАМ. - 2015. - №4.

57 Mumm, D. R. Characterisation of a cyclic displacement instability for a thermally grown oxide in a thermal barrier coating system [Text]/ D. R. Mumm, A. G. Evans and I. T. Spitsberg/ Acta Materialia. – 2001. – V. 49. – P. 2329–2340.

58 Schulz, U. Influence of substrate material on oxidation behaviour and cyclic lifetime of EB-PVD TBC systems [Text]/ U. Schulz, M. Menzebach, C. Leyens and Y.Q. Yang / Surface and Coatings Technology. – 2001. – V. 146-147. – P. 117-123.

59 Tolpygo, V. K. Morphological evolution of thermal barrier coatings induced by cyclic oxidation [Text]/ V. K. Tolpygo and D. R. Clarke/ Surface and Coatings Technology. – 2003. – V. 163-164. – P. 81-86.

60 Rabiei, A. Failure mechanisms associated with the thermally grown oxide in plasma-sprayed thermal barrier coatings [Text]/ A. Rabiei and A. G. Evans/ Acta Materialia. – 2000. – V. 48. – P. 3963-3976.

61 Evans, A.G. Mechanics-based scaling laws for the durability of termal barrier coatings [Text]/ A.G. Evans, M. Y. He and J. W. Hutchinson/ Progress in Materials Science. – 2001. – V. 46. – P. 249-271.

62 Wang, J. S. Measurement and analysis of buckling and buckle propagation in compressed oxide layers on superalloy substrates [Text]/ J. S. Wang and A. G. Evans/ Acta Materialia. – 1998. – V. 46. – P. 4993-5005

63 Абраимов Н.В. Высокотемпературные материалы и покрытия для газовых турбин [Текст]/Н.В. Абраимов. – М.: Машиностроение, 1993. – 336 с.

64 Тушинский, Л. И. Методы исследований материалов: Структура, свойства и процессы нанесения неорганических покрытий [Текст]/Л. И. Тушинский, А.В. Плохов, А.О. Токарев, В.И. Синдеев. — М.: Мир, 2004. - 384 с

65 Петрова, Л. Г. Современные методы исследования структуры и свойств диффузионных слоев после химико-термической обработки

[Текст]/Л.Г. Петрова, В.А. Александров, С.И. Барабанов//Вестник Харьковского национального автомобильно-дорожного университета. - 2011. - №54. - С.60-72.

66 Смирнов, А. А. Исследование влияния барьерного слоя на жаростойкость защитного покрытия для лопаток турбин высокого давления из сплава жс32 [Текст]/А. А. Смирнов, С. А. Будиновский//Труды ВИАМ. - 2017. - №1.

67 Глазов, В.М. Микротвердость металлов и полупроводников. Издание второе, исправленное и дополненное [Текст]/В.М. Глазов, В.Н. Вигдорович – М.: Металлургия, 1969. -248 с.

68 Vickers Hardness test [Electronic reference] /SCRIB.COM: Scrib, Inc.- 2016.-URL: https://es.scribd.com/document/295258890/6-Vickers-Hardness-Test (manipulation date: 04.05.2019).